

This paper not be be cited without prior reference to the author.

International Council  
for the Exploration of the Sea

C.M. 1975/C: 22  
Hydrography Committee

AN INTEGRATED APPROACH TO THE REMOTE SENSING OF FLOATING ICE

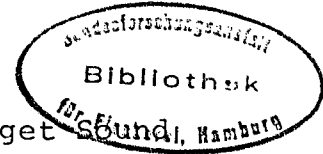
by

W.J. Campbell  
U.S. Geological Survey, University of Puget Sound,  
Tacoma, Washington 98416, U.S.A.

R.O. Ramseier  
Department of the Environment  
580 Booth Street  
Ottawa, Ontario, K1A 0H3, Canada

W.F. Weeks  
U.S. Army Cold Regions Research and Engineering Laboratory  
Hanover, New Hampshire 03755, U.S.A.

P. Gloersen  
NASA-Goddard Space Flight Center  
Greenbelt, Maryland 20771, U.S.A.



ABSTRACT

The current increase of scientific interest in all forms of floating ice - sea ice, lake ice, river ice, ice shelves and icebergs - has occurred during a time of rapid evolution of both remote-sensing platforms and sensors. The application of these new research tools to ice studies has generally been both piecemeal and sporadic, partly because the community of ice scientists has not kept up with the rapid advances in remote sensing technology and partly because they have not made their needs known to the space community. This paper seeks to help remedy the latter shortcoming. The remote sensing requirements for floating ice studies are given, and the capabilities in meeting these requirements are discussed. The desirable future sensors are also discussed from both the research and operational points of view.

## AN INTEGRATED APPROACH TO THE REMOTE SENSING OF FLOATING ICE

### 1. INTRODUCTION

Within the last few years there has been a sharp increase in the variety of satellite and aircraft borne remote-sensing techniques that show promise for the investigation of the floating ice covers of the world's oceans, lakes, and rivers, as well as shelf ice, and icebergs. Associated with this increase in technical capability there has also been an increase in actual remote sensing studies of ice-related problems (Campbell et al., 1975; Page and Ramseier, 1975). Many of these studies are, of course, focused on examining what a given sensor can and cannot detect. Two examples are, the recent studies of the variation of microwave signatures with changes in sea ice type (Wilheit et al., 1972; Gloersen et al., 1973; Ramseier et al., 1974) or the investigation of whether or not the intensity of a SLR (side looking radar) return can be used to indicate if a lake is frozen to its bottom (Sellman et al., 1975). Other studies focus on using a specific sensor to study a specific type of problem; for instance, the use of LANDSAT imagery to study ice drift and deformation (Hibler et al., 1975; Ramseier et al., 1975) or the use of IR imagery to estimate sea ice thickness (Poulin, 1973, 1975; Gloersen et al., 1974). Only a few studies have attempted to explore the potential of applying a set of varied remote sensing observations to resolving a problem, even though this

approach obviously has great promise (Campbell et al., 1974). The major current example of trying to utilize an integrated, multi-sensor remote sensing program as a fundamental input to a coordinated investigation of sea ice dynamics is presently underway in AIDJEX (Arctic Ice Dynamics Joint Experiment) (Weeks and Campbell, 1975). It is our experience with this project that has convinced us that in the future the great majority of floating ice problems will require data to be collected simultaneously by a variety of satellite-borne sensors. After all, it is only by remote sensing technology that the vast areas of the earth's surface covered by floating ice can be sampled on the large space-scales and short time-scales that are required.

## 2. REMOTE SENSING REQUIREMENTS

First we will discuss exactly what sort of information investigators who study the different types of floating ice would like to acquire and why. Here no attention will be paid to whether or not a remote sensing technique exists, or is likely to exist, that will collect the requisite data. A summary of the required information is given in Table 1 as is an estimate of the desired time and space scales involved. In the following it should always be kept in mind that in most floating ice problems extremely large expanses of ice are involved. Therefore, one will always be faced with the compromise between obtaining enough data to give adequate estimates of the parameter of interest and collecting so much data that processing becomes an intolerable

burden. This is particularly true when one considers the rapidity with which drifting ice may undergo significant changes.

## 2.1 Sea Ice

Of first importance is the need to sense the presence (or absence) of ice. This is essential for defining the edges of the ice pack which may assume rather complicated wave and stream type forms. It is also essential for sensing the presence of open leads within the pack. Although a horizontal resolution of 100 m is adequate to resolve most features along the ice edge, a higher resolution (taken here as 5 m) would be useful in delineating the many narrow leads/cracks that occur in the pack. At the present there are no studies of the relative contribution of narrow leads that are below the resolution of current satellite systems such as LANDSAT or NOAA, to the actual observed strains (see Figure 1). It is certainly conceivable (but doubtful) that many small unobserved leads may be as important as the few large leads that show clearly in the imagery.

Once the ice/open water distinction is made, it is necessary to give estimates of the areal amounts of ice of different thicknesses. These data coupled with the amount of open water specify the ice thickness distribution (G). At the present time G is believed to be the most important single parameter that controls the rheological response of pack ice to external forces (Thorndike et al., 1975). In this sense the critical end of the

ice thickness distribution is the thin ice portion since it is known that thin ice is invariably deformed before thicker older ice. In fact thick (3-4 m) multiyear ice is rarely deformed during ice drift. Therefore in Table 1 the recommended vertical resolution of 10 cm is particularly applicable to the determination of ice thickness in thinner ice (< 1 m). In thicker ice a vertical resolution of 25 to 50 cm would be adequate. The spatial resolution of 5 m is believed to be necessary in order to resolve the rapid local changes in thickness that are commonly caused by ridging and by the refreezing of newly formed leads. These striking thickness variations are well shown in Figure 2 which presents a portion to the sonar profile of the underside of the ice in the Arctic Ocean obtained by the British submarine HMS Dreadnought during its March 1971 cruise to the North Pole (Swithinbank, 1972). For many purposes monthly estimates of G should be adequate in areas with a heavy ice cover such as the Beaufort Sea, inasmuch as it is now possible to calculate the changes in G from existing ice drift and deformation models (Thorndike et al., 1975). Therefore, the observed G values would primarily be used to calibrate and check the model calculations. However, there are areas of thin first-year ice such as the Bering and Baltic Seas where more frequent (weekly) measurements of G would be desirable. This is particularly true during time periods when

burden. This is particularly true when one considers the rapidity with which drifting ice may undergo significant changes.

## 2.1 Sea Ice

Of first importance is the need to sense the presence (or absence) of ice. This is essential for defining the edges of the ice pack which may assume rather complicated wave and stream type forms. It is also essential for sensing the presence of open leads within the pack. Although a horizontal resolution of 100 m is adequate to resolve most features along the ice edge, a higher resolution (taken here as 5 m) would be useful in delineating the many narrow leads/cracks that occur in the pack. At the present there are no studies of the relative contribution of narrow leads that are below the resolution of current satellite systems such as LANDSAT or NOAA, to the actual observed strains (see Figure 1). It is certainly conceivable (but doubtful) that many small unobserved leads may be as important as the few large leads that show clearly in the imagery.

Once the ice/open water distinction is made, it is necessary to give estimates of the areal amounts of ice of different thicknesses. These data coupled with the amount of open water specify the ice thickness distribution (G). At the present time G is believed to be the most important single parameter that controls the rheological response of pack ice to external forces (Thorndike et al., 1975). In this sense the critical end of the

ice thickness distribution is the thin ice portion since it is known that thin ice is invariably deformed before thicker older ice. In fact thick (3-4 m) multiyear ice is rarely deformed during ice drift. Therefore in Table 1 the recommended vertical resolution of 10 cm is particularly applicable to the determination of ice thickness in thinner ice (< 1 m). In thicker ice a vertical resolution of 25 to 50 cm would be adequate. The spatial resolution of 5 m is believed to be necessary in order to resolve the rapid local changes in thickness that are commonly caused by ridging and by the refreezing of newly formed leads. These striking thickness variations are well shown in Figure 2 which presents a portion to the sonar profile of the underside of the ice in the Arctic Ocean obtained by the British submarine HMS Dreadnought during its March 1971 cruise to the North Pole (Swithinbank, 1972). For many purposes monthly estimates of G should be adequate in areas with a heavy ice cover such as the Beaufort Sea, inasmuch as it is now possible to calculate the changes in G from existing ice drift and deformation models (Thorndike et al., 1975). Therefore, the observed G values would primarily be used to calibrate and check the model calculations. However, there are areas of thin first-year ice such as the Bering and Baltic Seas where more frequent (weekly) measurements of G would be desirable. This is particularly true during time periods when

the frequent passage of cyclones causes pronounced ice deformation.

If sea ice were in local isostatic equilibrium then accurate measurements of ice thickness coupled with a knowledge of the density of the ice would specify the roughness of both the upper and lower ice surfaces. However it is known that in the vicinity of pressure ridges pronounced local deviations from isostatic equilibrium are common (Weeks et al., 1971). Therefore, it is desirable to measure the roughnesses of both ice surfaces independently so that any changes in these values can be incorporated into changes for the estimated surface drag coefficients for wind and water. Figure 1 shows a laser profile of the upper side of the ice. In ridged areas the changes in roughness are striking. Current information (Hibler, 1975) suggests that although a vertical resolution of 10 cm is desirable in measuring ridge sails, a resolution of 1 m is probably quite adequate for ridge keels. One problem associated with adequately measuring roughness, is that currently available techniques (laser, sonar) provide profile measurements, while, in fact, what is needed is the characterization of the roughness of broad areas. Fortunately during most periods of the year roughness is not believed to change rapidly. The principal exception to this is probably the early portion of the melt season when ablation rapidly rounds the jagged sails of first-year ridges.

It is also desirable to be able to categorize sea ice depending upon its physical characteristics. The most obvious sub-groups here would be first-year ice (thickness < 2 m, 5 to 15‰ salinity) and multiyear ice (thickness between 2 to 4 m, 0 to 4‰ salinity). This pronounced difference in salinity is caused by the extensive brine drainage and flushing of nearly fresh water through the ice during the summer melt period. Therefore multiyear ice and multiyear pressure ridges are much stronger than first-year ice because of the lower brine volume resulting from the lower salinity. The first-year/multiyear separation is also a useful one in that multiyear ice to a large degree forms the "undeformable" matrix within which first-year ice grows and is deformed.

Even better than the first-year/multiyear ice distinction would be to directly measure some pertinent physical characteristic of the ice, either as an average value such as the average salinity or even better as a profile. In thin ice a 10 cm vertical resolution of the property being profiled is desirable while in thicker ice a 50 cm resolution would be adequate. The most important single parameter that could be measured to specify the mechanical, electrical and chemical characteristics of sea ice is the brine volume profile which in turn is specified by the salinity and temperature profiles (Weeks and Assur, 1969). Measuring the temperature profile or at least the ice surface temperature is also very important in estimating

the ice growth rate and the surface heat balance of the ice. The principal problem in relating variations in the snow surface temperature to variations in ice thickness is caused by the snow cover on the ice. Inasmuch as there is no simple relation between time and snow thickness one cannot in general use surface temperatures as determined by satellite-borne radiometers to make estimates of the temperature of the underlying ice without independent information on the characteristics of the snow cover (Poulin, 1975). The principal exception to this is found in thin newly formed ice which because of the brief period between its formation and the time of observation usually has not accumulated an appreciable snow cover. Fortunately it is this thin ice and the areas of open water that are of prime importance in specifying the thermal exchange between the ocean and the atmosphere in the Arctic. Note that in Table 1 two different scales are designated as of interest in studying both the surface heat flux and the surface albedo: the 10 km or larger scale which would be of interest for regional studies, and the 100 m scale which is needed if one wishes to examine specific uniform ice types and/or conditions. The frequency of measurement required for either meso- or macroscale heat flux studies would be daily because of the possibility of the rapid opening or closing of systems of leads.

Information is also needed on the drift and the deformation of the pack as well as on the general geometry of the floes and

leads. Typical drift velocities within the pack are roughly 5 km/day (Dunbar and Wittmann, 1963). The largest values (up to 20 km/day) are invariably found near the free edge of the pack where no lateral constraint exists on the ice movement. Strains within the ice as large as several percent are commonly noted, and are associated with the passage of a cyclone through or near the area of interest. Associated with these strains differential motions along highly oriented systems of leads are commonly observed. Because one system of leads may close (or become inactive) while another system rapidly forms, it is desirable to have information on these changes collected at least daily.

Finally a parameter of particular importance to shipping interests is the state of divergence in the ice pack - whether it is increasing or decreasing. Converging ice is difficult or impossible to negotiate even with an ice breaker, whereas diverging ice presents little impediment to a properly designed vessel.

## 2.2 Lake and River Ice

As noted in Table 1, the problems encountered in the study of lake and river ice are quite similar to those encountered in sea ice. This is particularly true in fresh water bodies in which a continuous fixed (fast) ice cover does not form and the ice continues to drift during the period of ice growth.

The principal differences, when contrasted with sea ice, are that the ice that is formed does not have an appreciable

salinity. However, pronounced layers of entrapped air bubbles that can serve as scattering centres are quite common. It also should be remembered that inasmuch as the dielectric loss is lower in fresh water ice than it is in sea ice, electromagnetic radiation can penetrate through quite thick layers of fresh ice. Because of this the internal properties of the ice are important in determining the nature of the return signal when radar or microwave techniques are used. Details of which specific aspects of the ice are important are, however, many times poorly understood.

Two particular problems that are unique to rivers are the occurrence of frazil ice crystals in turbulent water and ice jams at constrictions in streams. It would, of course, be of interest to be able to sense both of these phenomena. It should be remembered that although the resolution requirements for most lake ice studies are similar to those for sea ice, many river ice problems require a significantly higher resolution inasmuch as it is the constrictions in a river which may only be a few tens of meters wide that are commonly of interest.

### 2.3 Shelf Ice and Icebergs

In general the information that is required in the study of ice shelves is surprisingly similar to that required for pack ice. The time scales are, however, quite different in that, with the exception of surface heat flux which would be required daily, most observations are required either quarterly or yearly. This

reduces the amount of data processing. It should, however, be noted that although the items of interest are similar, the values that would be measured are quite different as are the processes involved (Swithinbank and Zumberge, 1965). For instance, ice shelf thicknesses vary from 100 to 500 m; the small scale roughness of the upper shelf surface is primarily the result of aeolian processes as contrasted with pressure ridges; the ice itself is primarily glacier ice or superimposed snow ice; and the salinity is due to lateral percolation of brine from the seaward edge of the shelf or from crevasses that permit the entry of sea water. Typical ice velocities on Antarctic ice shelves are 500 m/year. There are also pronounced variations in these velocities associated with the presence of faster flowing ice streams within the shelves.

Icebergs are primarily of interest as hazards to be avoided by shipping although it is conceivable that at some future time they may be utilized as a fresh water source (Weeks and Campbell, 1973). It is necessary to accurately keep track of icebergs within shipping lanes until melting has reduced them to quite small sizes. Because iceberg drifts in the open ocean can be rapid it is not necessary to know their positions more accurately than 1 km at any given time of sensing. If there are features that allow the identification of specific icebergs, then their paths can be studied and analyzed in terms of the different forces that are involved.

### 3. SENSOR CAPABILITIES

Here we will briefly discuss the capabilities of a number of satellite systems that are either currently operational or presumably will be so in the near future. When possible we will also give references where more detailed information can be found. The characteristics of the sensors that are discussed are summarized in Table 2.

#### 3.1 Visible and Near Infrared

##### 3.1.1 LANDSAT

LANDSAT (formerly known as ERTS) imagery is of cartographic quality on a scale of 1:10<sup>6</sup>. Each image is 185 km on a side. The Multi-Spectral Scanner (MSS) sensor system collects information in 4 spectral bands ranging from visual (0.5  $\mu\text{m}$ ) to near IR (1.1  $\mu\text{m}$ ) with a stated surface resolution of 100 m. Experience has, however, shown that high contrast linear features such as leads with widths significantly smaller than this are commonly visible in the imagery. For instance, compare the LANDSAT imagery shown in Figure 1 with the U-2 imagery shown in the same figure. The imagery reveals a wealth of sea ice information and shows quite clearly the distinction between water and ice, the different classes of thin ice (< 50 cm) as opposed to thicker ice, the presence of melt ponds, of brash ice, and in some cases the difference between old and first-year ice (Barnes and Bowley, 1974; Barnes et al., 1975). Because of its scale, resolution, and map-like accuracy LANDSAT imagery is ideally

suites for studying lead patterns, ice drift and deformation. It is now being used as the basis for several such investigations (Hibler et al., 1974; Nye, 1975; Rothrock and Hall, 1975). There are, of course, a number of common ice features that cannot be distinguished on LANDSAT imagery (ridges, hummocks, rafted ice, individual melt features, and in most cases old ice).

The drawbacks of the LANDSAT imagery are that the MSS is limited by cloud cover. It is also limited by darkness although present indications are that highly useful data can be obtained at much lower light levels (sun angles) than those at which the satellite is normally operated. Also the latitude and longitude of the centre of each image as calculated from the satellite orbit have been shown to contain significant errors (up to 8 km difference between the real and the stated position). This induces uncertainties in the utilizations of LANDSAT to study ice drift at sites far from land, although average daily drift rates commonly exceed these uncertainties. Problems can also be encountered in calculating strains and vorticities because of the errors in estimating the orientation of the longitude lines. These problems have been discussed by Hibler et al., (1975) and a procedure for minimizing them has been developed.

The major drawback inherent in LANDSAT imagery is its lack of continuity. At the equator LANDSAT images exactly the same area once every 18 days. In the polar regions the orbital overlap permits coverage of the same site during 3 to 5

consecutive days (depending on the latitude) followed by a 13 to 15 day "holiday" before the satellite returns to the study area. When the days lost because of cloud cover are added to these "holiday" periods, LANDSAT coverage has, in fact, proven to be quite spotty. To obtain the optimum use of LANDSAT identifiable ice features must be located on sequential images. The long holiday periods make this identification difficult except during periods of exceptional weather which of course, are not periods of storm passage when most interesting changes occur in the ice pack. Nevertheless, even with these drawbacks, LANDSAT imagery has, because of its cartographic quality and good resolution, proven to be the current satellite system that is presently most useful for quantitative studies of ice drift and deformation.

### 3.1.2 NOAA

The NOAA satellite series has also produced a large amount of imagery that is useful in the study of sea ice (McClain, 1974 (a) and (b)). These satellites operate at appreciably higher altitudes than do satellites in the LANDSAT series (1465 km above the earth's surface as compared with 900 km). The prime sensor involved for sea ice studies is a dual channel very high resolution radiometer (VHRR) which obtains information in both the visible (0.5 - 0.7  $\mu\text{m}$ ) and the infrared (10 - 12.5  $\mu\text{m}$ ) regions. The images produced are 2000 km on a side and have a surface resolution of 1 km. In the polar regions a given area is usually imaged once daily. These satellites also carry a

scanning radiometer that gives a twice daily image of any location on the earth's surface in both the visible and IR but at a reduced resolution (8 km). It is also possible to enhance the resulting imagery by distributing the 16 distinguishable grey tones over the 30 degree temperature range usually encountered in the Arctic as opposed to the 100 degree range commonly utilized for meteorological purposes.

The advantages of NOAA imagery are that during both light and dark periods, it provides regular broad scale coverage of the polar regions on a scale at which many useful large ice features can still be distinguished. The disadvantages are that images cannot be obtained through a cloud cover, the resolution and scale are sufficiently large so that many interesting and important ice features are lost (for instance in Figure 1 compare the NOAA image with the LANDSAT image and the U-2 photograph), and finally the projection of the image is such that quantitative drift and deformation measurements are difficult.

At the present, most sea ice studies based on NOAA imagery have been semi-quantitative analyses of the regional behaviour of pack ice areas such as the Beaufort and Bering Seas and the Southern Ocean (Ackley and Hibler, 1975; Stretten, 1974; DeRycke, 1973). If the data could be displayed in a format that would facilitate quantitative ice drift and deformation measurements, it would definitely enhance the usefulness of the imagery to the sea ice community.

### 3.1.3 DMSP (Defense Meteorological Satellite Program)

This satellite series which was formerly called DAPP (Data Acquisition and Processing Program) is operated by the U.S. Air Force for the U.S. Department of Defense. The principal purpose of the satellites is the observation of cloud patterns. The imagery is collected by both high resolution and very high resolution 2 channel radiometers operating in both the visual (0.4 to 1.1  $\mu\text{m}$ ) and the IR (8 to 13  $\mu\text{m}$ ) ranges. The satellites orbit at a slightly lower altitude (833) than satellites in the LANDSAT series and significantly lower than those in the NOAA series. Usually two DMSP satellites are in orbit at the same time which provides coverage of any spot on the earth's surface four times daily. The VHRR system which is of primary interest here has a spatial resolution of 0.61 km at nadir. The imagery is currently archived at the University of Wisconsin Space Science and Engineering Center. A detailed description of the satellite system is given by Dickenson et al., (1974). DMSP imagery provides a view of sea ice on a scale that is intermediate between that of LANDSAT and of NOAA. Several images are obtained each day, darkness is not a limitation, and the map format, while not as convenient as LANDSAT, is easier to use than NOAA. In addition there are a variety of options available for specially processing both the visual and the IR data, so that the imagery has a higher apparent resolution and the temperature (or albedo) scale is expanded relative to some arbitrarily set base

value such as the freezing temperature of sea water. Figure 3 shows the ice north of Alaska presented in such an expanded format. Note the large amount of detail that is revealed about the lead structure within the pack. This type of specially processed data will apparently be available on a routine basis in the fall of 1975. The principal limitations of the sensing system are that it does not penetrate clouds and does not possess as high a spatial resolution as might be desired.

### 3.2 Thermal Infrared

As discussed in the previous sections both the NOAA (and its predecessor ITOS) and the DMSP satellites have thermal IR systems operating respectively in the ranges of 10.5 - 12.5  $\mu\text{m}$  and 8 - 13  $\mu\text{m}$  and with resolutions of 1.0 and 0.6 km. Other satellites with IR systems of interest are in the NIMBUS series. The High Resolution Infrared Radiometer (HRIR) systems on NIMBUS 1, 2 and 3 operated in the 3.4 to 4.2  $\mu\text{m}$  window which was only useful at night because of contamination by reflected solar radiation during daylight hours. The approximate spatial resolution at nadir was between 3.3 and 7.4 km. On NIMBUS 2 and 3 the HRIR system was joined by a five channel medium resolution system (MRIR) that operated in a scanning mode with a ground resolution of approximately 55 km at the subpoint. On NIMBUS 4 the HRIR and MRIR systems were replaced by a Temperature Humidity Infrared Radiometer (THIR) experiment that was designed to provide both day and night cloud and surface temperature information as well

as information on the moisture content of the upper troposphere and stratosphere. The THIR system had a ground resolution of 7 km for the temperature channel. NIMBUS 5 was equipped with a Scanning Microwave Radiometer with 3 detectors of which the thermal IR operated at a wavelength of 10.5 to 11.3  $\mu\text{m}$  with a resolution of 0.8 km. NIMBUS G will also fly a scanning radiometer operating in a similar range (10.5 to 12.5  $\mu\text{m}$ ) with a resolution of 0.8 km.

While the list of satellites and radiometers is rather overwhelming the trend is clear. The first IR sensors were only useful at night and had a low resolution while the more recent versions operate successfully either during the day or night with increasing resolution. Because of their resolution limitations the IR systems on the early satellites were primarily useful for the mapping of gross ice boundaries such as the edge of the pack or the location of large polynyas (Barnes et al., 1972). Even as the resolution of the IR systems improved to values of 1 km or less so that detailed observations of features within the pack became possible, little was done with the IR imagery except use it during dark periods as a replacement for visual imagery which was usually of an even better resolution. This was done by simply noting that open water or thin ice areas that appeared dark on visual imagery (low albedo) also appeared warm on the IR imagery. However, these studies indicated that the large reflectance changes that made the water-ice transition so clear

in the visual range often corresponded to much less obvious thermal contrasts as recorded by the IR system. This was particularly true when the IR image was displayed by distributing the distinguishable grey shades over the 100°C of interest for meteorological purposes. It was the problem of improving these sorts of contrasts that stimulated the development of the special enhancement techniques that are now being applied to both the IR and visible imagery from the NOAA and DMSP satellites.

Admittedly Poulin's (1975) cautions concerning the difficulties introduced in the quantitative interpretation of snow (usually of unknown thickness and density) are quite correct and should be heeded by all considering studies in this field. Nevertheless it is our opinion that there will prove to be considerable profit in quantitative studies of regions of thin ice (with presumably thin snow covers) via IR techniques alone or, if possible, IR coupled with other techniques. Examples of such recent studies are Barnes et al., (1972) and Chase (1972).

Table 1. Desired Remote Sensing Capability for Floating Ice.

Parameter to be Measured	Maximum Desired Resolution (H = horizontal, V = vertical)	Minimum Usable Resolution	Frequency of Observations
<u>1. Sea Ice</u>			
Presence or absence of ice	5 m (H)	100 m (H)	Daily
Ice thickness	10 cm (V), 5 m (H)	1 m (V) 25 m (H)	Weekly
Roughness of upper and lower surfaces	10 cm (V), 1 m (H)	10 cm (V), 5 m (H)	Monthly
Ice type characterization	5 m (H)	100 m	Monthly
Ice temperature	10 cm (V), 5 m (H)	10 cm (V), 100 m (H)	Weekly
Ice salinity	10 cm (V), 5 m (H)	10 cm (V), 100 m (H)	Weekly
Ice and lead patterns	5 m (H)	100 m (H)	Daily
Ice concentration	5 m (H)	0.1-25 km (H)	Daily
Ice drift	± 50 m	0.1-25 km (H)	Daily
Ice deformation	± 0.1%	± 0.1%	Daily
Surface albedo			
regional	10 km	100 km	Weekly
local	100 m	1 km	Weekly
Surface heat flux			
regional	10 km	100 km	Daily
local	100 m	1 km	Daily
<u>2. Lake Ice</u> - same as above, except for salinity which is not applicable.			

3. River Ice - again the factors are similar to those given for sea ice (deleting ice salinity). Because of the extremely dynamic nature of many river ice covers, ice roughness should probably be measured weekly.

4. Shelf Ice

Ice thickness	5 m (V)	Same	Yearly
Roughness of upper and lower surfaces	upper 10 cm (V), 1 m (H); lower 1 m (V), 10 m (H)	Same	Yearly
Ice type characterization	5 m (V), 100 m (H)	5 m (V), 0.1-25 km (H)	Yearly
Ice temperature	5 m (V), 100 m (H)	5 m (V), 0.1-25 km (H)	Monthly
Ice salinity	5 m (V), 100 m (H)	5 m (V), 0.1-25 km (H)	Yearly
Crevasse patterns	100 m (H)	Same	Yearly
Ice motion	± 10 m (H)	± 100 m (H)	Quarterly
Ice deformation	± 0.1%	Same	Quarterly
Surface albedo	10 km (H)	100 km (H)	Quarterly
Surface heat flux	10 km (H)	100 km (H)	Daily
5. <u>Icebergs</u>			
General dimensions	5 m	Same	Weekly
Location	1 km	Same	Daily
Any geometric or internal characteristics that would allow one to trace the motion of specific icebergs		Same	Daily

### 3.3 Passive Microwave

Perhaps the most rapidly evolving area of remote sensing research in floating ice has been in passive microwave applications. Both aircraft and satellite-borne microwave radiometers have been used to observe a wide variety of ice types during the last five years. Although the time span is short, sufficient data now exists to cause us to conclude that such measurements will be a fundamental part of future ice observation programs.

#### 3.3.1 Aircraft Microwave Observations

The most important series of aircraft flights which demonstrated the feasibility and usefulness of ice observations by means of passive microwave sensors were those that occurred during the NASA-AIDJEX (Arctic Ice Dynamics Joint Experiment) program and the U.S./U.S.S.R. BESEX (Bering Sea Experiment) joint program. A series of three AIDJEX pilot field experiments were performed during the springs of 1970, 1971, and 1972 in the southern Beaufort Sea. During each of these experiments, the NASA CV-990 "Galileo I" performed a variety of flights ranging in altitude from 150 m to 11 km. A wide variety of visual and infrared sensors were operated in addition to a 19.3 GHz imaging radiometer and 1.42 GHz, 4.99 GHz, 10.75GHz and 37.0 GHz radiometers.

The 1970 data (Wilheit et al., 1971, 1972) showed that it was possible to distinguish sea ice from liquid water both

through the clouds and in the dark. This finding was exciting because it pointed the way to an "all-time" ability to observe leads and polynyas. These data also showed that strong microwave emissivity differences occur on the ice surface itself. However, the lack of sufficient ground truth data prevented a determination of the reason for these differences.

The ground truth measurements and mesoscale microwave mosaic maps (10,000 km<sup>2</sup>) acquired during the 1971 AIDJEX-NASA experiments allowed Gloersen et al., (1973) to show that the observed emissivity differences of sea ice at a frequency of 19.35 GHz are associated with the age of the ice, with multiyear ice having cold brightness temperatures (~210°K) and first-year ice having warm ones (~235°K). This was an important breakthrough because it suggested that passive microwave imagery could provide an all-time capability of distinguishing between old (thick) and new (thin) ice and of tracking ice motion as well as lead and polynya dynamics. Figure 5 shows a 19 GHz microwave image from that paper depicting the observed emissivities of a large ice area (10,000 km<sup>2</sup>) of the eastern Beaufort Sea. The multiyear floes, having an average thickness of 3-4 m, have cold (blue) brightness temperatures while the warm (yellow) temperatures are associated with first-year floes having average thicknesses of less than 2 m.

During the 1972 AIDJEX-NASA experiment two experimental innovations were made: a sled mounted 13.4 GHz microwave

radiometer was used to map in detail the surface brightness temperatures of areas of various ice types where detailed crystallographic measurements had been made, and during each of the seven flights a mosaic microwave image was obtained of a segment of the southern margin of the ice cover adjacent to the north coast of Alaska. Analysis of the surface truth data by Meeks et al., (1974) showed that surface salinity and pore size were primarily responsible for determining the microwave signatures of sea ice of various ages. It also showed that for mixtures of ice of different ages in which the floes are smaller than the radiometer footprint, the percentage of first-year versus multiyear ice can be estimated using microwave techniques. Figure 5 also shows a microwave image of the 1972 AIDJEX area in the western Beaufort Sea. A comparison of this image with one obtained a year earlier in the eastern Beaufort Sea reveals a markedly different morphological makeup of the ice in that no large multiyear floes were present. Campbell et al., (1975) noted that numerous small multiyear floes, smaller than the radiometer footprint of 500 m, were observed in the area, and by matching and averaging radiometer signatures of the various ice types they found that the 1972 AIDJEX area was made up of approximately equal amounts of multiyear and first-year ice.

The AIDJEX-NASA pilot experiments showed that microwave imagery can be used to study the morphology and dynamics of ice at the edge of the ice pack as well as ice within the pack. A

time sequence of microwave mosaic images of the sea ice extending from Harrison Bay, on the northwest of Alaska, north into the Beaufort Sea for 350 km is shown in Figure 6. The seven images cover the time from 4 to 23 April 1972. Three distinct zones of sea ice can be observed in each image: (1) a shore-fast zone made up of undisturbed first-year ice having a uniformly high brightness temperature; (2) a shear zone composed of three distinct ice types - multiyear floes with cold brightness temperatures, refrozen polynyas with brightness temperatures similar to those of shore-fast ice and a mixture of first-year and unresolvable chunks of multiyear ice having a brightness temperature between those of the two ice types; and (3) a zone of a mixture of first-year and unresolvable floes of multiyear ice with many refrozen polynyas. The extremely dynamic nature of the shear zone is clearly seen, with its width doubling in 19d.

During the U.S./U.S.S.R. BESEX experiment in April 1973, the "Galileo I" obtained four mesoscale microwave images (10,000 km<sup>2</sup>) of parts of the Bering Sea ice pack at the time of its maximum extent. The pack ice in this region is quite unlike that of the Beaufort Sea in that it is all first-year ice, with thicknesses ranging from a few centimetres to a metre. In addition, this ice is subject to rapid dynamic changes because it is unbounded on its southern edge. Actually the Bering Sea ice pack more closely resembles the Antarctic ice pack than the ice pack of the Arctic Ocean. Figure 7 shows the 19 GHz image for 20 February 1973

(Gloersen et al., 1974) with a N-S orientation of polynyas that had formed as the pack drifted rapidly southward during the preceding six days. The amount of open water indicated by this image is 16%.

During April and August 1975, the "Galileo II" performed a variety of missions in conjunction with the Main AIDJEX experiment, which involves an array of four manned drifting stations and eight unmanned data buoys drifting from March 1975 until May 1976 in the Beaufort Sea. Similar flights will also take place in October 1975 and April 1976. The data from these missions is being used to help interpret satellite imagery of the ice pack and as input into numerical models of the pack.

Microwave images of lake ice acquired from aircraft (Ramseier and Gloersen, in press) in most respects resemble those of young sea ice in that the ice emits a warm signature and can clearly be distinguished from open water. The exception is that very thin lake ice emits various signatures because penetration is occurring and the Fabry-Perot effect takes place. For ice thicknesses less than five times the wavelength, the emissivity oscillates from close to zero to unity as thickness changes by  $\lambda/4$ , therefore a wide range of signatures can be emitted by thin ice.

### 3.3.2 ESMR

The Electronically Scanning Microwave Radiometer (ESMR) on NIMBUS-5 has provided the first large-scale synoptic views of the

polar sea ice packs. These have been interpreted in light of the AIDJEX-NASA and BESEX findings revealing that both the morphology and dynamics of these major ice masses are more complex than had hitherto been assumed. Since its launch on 11 December 1973 NIMBUS-5 has provided a wealth of data on the variations of these packs at time scales ranging from several days to seasons. Figure 8 shows a pair of ESMR images of the Arctic at different seasons. The winter image of 11 January 1973 shows the ice canopy to be composed of two general types of ice: the principally multiyear ice covering the main portion of the Arctic Ocean, with brightness temperatures ranging from 209 to 223°K, and either first-year or first-year/multiyear mixtures with higher brightness temperatures covering the southern portion of the marginal seas (i.e. the Beaufort, Chukchi, East Siberian, Laptev, Kara and Barents Seas). Note that the multiyear ice extends far south into the eastern Beaufort Sea. By using a combination of ESMR and LANDSAT-1 images combined with the AIDJEX-NASA data, Campbell et al., (1974) have shown that the Beaufort Sea ice cover is made up of large multiyear floes in its eastern sector while its western sector consists of small, fragmented first-year and multiyear floes.

By the end of the summer melt season the ESMR image for 8 September 1973 (Fig. 8) shows that most of the ice that had covered the marginal seas had melted. The area of the end-of-summer pack is approximately half of that of the winter pack.

Analysis of these and other ESMR images by Gloersen et al., (1974) reveals that not all of the first-year/multiyear ice mixture melted. Figure 9 shows an analysis of the near-maximum ice extent (10 February 1973) and near-minimum ice extent (9 September 1973) based on the ESMR images. The areas of the pack in which the first-year/multiyear ice mixture survived the summer melt are source areas for multiyear ice which is advected into the multiyear pack. This process thereby, allows the ice pack to maintain a steady-state mass by balancing the volume of ice that is advected out of the Arctic Ocean by the East Greenland current. The analysis also shows that the summer pack extended closer to Svalbard than did the winter pack, suggesting a strong summer ocean surface current flowing southward in this region. Gloersen et al., (1974) also show how the ice concentration can be inferred from ESMR images using a linear interpolation between the emissivity for open water and that of first-year ice. Note that the ESMR image for the Arctic in the winter of 1973 (Fig. 8) shows that the ice cover of the Bering Sea, which we have shown was made up of first-year and younger ice, has a cold radiometric signature similar to that of the multiyear ice of the Arctic Ocean. The reason for this is that the large (32 km) footprint of ESMR is covering a mixture of ice and open water, and the average brightness temperature appears cold because the water signature is much colder than that of the first-year ice.

Another parameter that can be inferred from a series of ice concentration measurements is the state of divergence of the ice, since increasing concentration with time implies a converging ice pack and decreasing concentration implies divergence.

The ESMR images of the Antarctic are equally useful as those of the Arctic for studying large-scale ice morphology and dynamics. Figure 10 shows both a winter and summer image of the Antarctic. The winter image indicates that the ice cover is made up exclusively of first-year ice. By late in the following melt season (10 February 1973), the ESMR image indicates that approximately 80% of the ice cover has melted. This is shown in the analysis given in Figure 11 in which the near-minimum (10 February 1973) and near-maximum (16 July 1973) ice extents are delineated. The observations at first seem to indicate the formation of multiyear ice where ice remains at the end of the melt season. Analysis of ESMR images in Austral Spring 1972 and Austral Winter 1973 by Gloersen et al., (1974) indicate that no multiyear ice was present, thus the regions where ice remains at the end of the melt season are accumulation regions in a system of steady depletion and replenishment.

One striking feature appearing on all the ESMR images is that the edge of an ice pack is quite irregular, unlike the ice-pack boundaries shown in the atlases. The same disparity between the images and the atlases exists in regards to ice concentration, especially for the Antarctic where the images show

very small concentrations in many areas. Of course when we realize that an ESMR view is essentially synoptic while the curves shown in atlases result from statistical smoothing of many seasons of piecemeal data, we should not expect them to agree. The ESMR images allow us to observe sea ice behaviour over large space scales and will thereby permit us to test dynamic rather than statistical models.

ESMR images of lake ice show the onset of freezing and melting but are of limited use for ice morphology and dynamic studies because of the large (32 km) footprint. The same can be said for river ice.

ESMR images of shelf ice, such as the Ross Ice Shelf, have been shown by Chang et al., (1975) to give valuable data on the accumulation rate of the surface snow cover. These measurements when coupled to similar sequential ones of the ice cap from which the shelves flow should give very valuable data on variations of snow accumulation patterns and amount that are impossible to obtain by in situ surface measurements due to the immense logistical costs.

### 3.3.3 SMMR

The Scanning Multichannel Microwave Radiometer (SMMR) to be flown on SEASAT-A and NIMBUS-G has great potential application to floating ice research. The five imaging radiometers - 6.6 GHz, 10.69 GHz, 18.0 GHz, 22.05 GHz, and 37.0 GHz - will perform all

the measurements of the 19.35 GHz ESMR on NIMBUS-5 and the 37.0 GHz ESMR in NIMBUS-6.

For sea ice observation the multifrequency capability of SMMR will help considerably in distinguishing between multiyear ice and first-year ice with unresolvable amounts of open water, both of which have similar radiometric signatures in the 19 GHz ESMR images. Multifrequency images of the same area will permit the observer to distinguish between these ice types because the brightness temperature differences between water and ice and between new ice and old ice vary as a function of frequency.

All forms of floating ice commonly have snow covers. The amount of snow is a prime determinant of the energy balance in the ocean-ice-atmosphere system. By comparing multifrequency simultaneous images of floating ice the snow accumulation rates can be measured. Successive measurements from the onset of the accumulation season can give the total snow cover. Both of these measurements have never been made over most of the earth's floating ice.

#### 3.4 Active Microwave Sensors

The active microwave sensors, such as side-looking airborne radars and scatterometers, operate normally at wavelengths between 0.08 and 0.25 meters. This permits the electromagnetic radiation to penetrate fog, rain, snow, darkness, and cloudy weather, i.e. they are all-weather, day and night systems.

The parameters that the radars sense on the ice surface are its dielectric properties and roughness. A certain amount of electromagnetic radiation is reflected from the surface, and the remainder penetrates the ice. The penetration of the radar wave into the ice is limited by the salinity of the ice and by discontinuities such as airbubbles, brine pockets and channels near the surface.

#### 3.4.1 Side-Looking Radar (SLR)

The SLR transmits electromagnetic radiation from an antenna mounted on an aircraft with its beam looking in a fixed sidewise direction at right angles to the aircraft track. Scanning is achieved by the forward motion of the aircraft so that the radar image obtained is in a cartesian format relative to the aircraft flight path. The intensities of the received radar echoes are usually recorded on a continuous strip of film.

There are two basic SLR systems which differ markedly in the image resolution obtained. The simplest type is the non-coherent or real-aperture SLR, in which the azimuthal, or along-track, resolution is determined by  $\lambda R/L$  where  $R$  is the range,  $L$  is the aperture of antenna and  $\lambda$  is the wavelength. The range resolution, or across-track resolution, is determined by the pulse duration or band width. To obtain a higher azimuthal resolution the antenna beam width would have to be decreased, resulting in a much longer antenna, which would make it

impractical for mounting on an aircraft, or the wavelength or range could also be changed.

It is also possible to use the motion of the aircraft itself to generate a long "synthetic" antenna. This second, more complex and costly type of radar is the coherent synthetic aperture system (SAR). By illuminating a small ground element by many successive radar pulses and recording the phase and amplitude of the returns, one may, after suitable processing, obtain an image of the ground element with a much higher resolution. The best possible along-track resolution for a focused SAR is independent of range and decreases as the real antenna is made shorter. For an unfocused SAR the resolution has a quadratic dependence on  $\lambda$  and  $R$  ( $\approx \sqrt{\lambda R}$ ). Even though the theory predicts that the resolution is half the real antenna length, this resolution is limited in practice by unavoidable perturbations in the flight path of the aircraft which restrict the time over which the signal phase history can be processed to produce the image.

Several studies of the application of such radars to the investigation of floating ice have been reported in the literature have been reviewed by Page and Ramseier, (1975) and Campbell et al., (1975). Since these papers have been written, the main AIDJEX experiment has commenced, yielding new and interesting results. Figure 12 shows a real aperture SLR image of the AIDJEX 1975 Big Bear area. The camp can be identified as

the black area near the centre of the image. Rough features appear dark in this image while smooth areas are light. The light linear features represent refrozen leads. All leads are covered with varying thicknesses of grey ice. Just north of and adjacent to the camp, the white linear feature running east-west represents the runway, consisting of 1.6 m thick first-year ice. The camp is located on a small multiyear ice floe having an average thickness of 3.5 m. The dark lines within this floe represent ridges having a height of approximately 2 m and a width of 3 m. The large lead which runs from northwest to southeast consists of grey ice with a thickness of 0.7 m. One aspect which is striking in this image concerns the backscattering coefficient  $\sigma$ . For example, the radar returns (grey scale) for the multiyear ice on which the camp is located and the large lead to the west of the camp are very much alike. If it would not be for the geometry of the ice, one could not distinguish first-year from multiyear ice. This is of great concern, since one of the future goals is to be able to automatically process digitized SLR data to obtain percentages of first-year and multiyear ice. The wavelike pattern on the west side of the camp running north-south is due to the aircraft motion. There is no question, however, that the information content of this SLR image is significant. For example, there was a relatively thick snow cover ( $\sim 0.20$  m) over the first and multiyear ice. The grey ice was snow-free.

The geometrical features of ice floes, leads, ridges, rubble ice fields, rafting in grey ice, are very distinct.

Figure 13 shows a SLR image of the MacKenzie delta area. The light tone on the south side represents shore-fast ice, followed in the north with the distinct shore-fast ice-pack ice boundary. The darker, rounded areas within the shore-fast ice represent stranded pieces of multiyear ice which are snow-covered. These pieces of multiyear ice are not visible in the aerial photography taken over the same area. The large floe in the centre of the image is multiyear ice. A lead running from the southwest to the northeast contains some grey-white ice (the darker area) and newly formed thin grey ice (light area) both of which are of varying thicknesses due to rafting. The northern part of the pack ice consists almost entirely of ridged first-year ice.

Figure 14 shows a number of frozen fresh water lakes in the vicinity of Barrow, Alaska. Sellmann et al., (1975) have shown that the difference in the backscatter from the tundra lakes indicates whether or not the lake is frozen completely to the bottom. The "dark" lakes (which here indicates low backscatter) do freeze completely to the bottom, whereas the "light" lakes (high backscatter) have an ice-water interface. The ability to differentiate via SLR between lakes that are fresh and not frozen to the bottom and lakes that are either frozen to their bottom and/or are brackish is of considerable economic, scientific and

engineering interest. For example, one could determine if: a given lake was suitable as a year-round source of water; should be considered for possible fishing or for stocking with fish; or should be considered as a site where permafrost may be deeply thawed due to the thermal effect of the year-round presence of a water body.

SLR imagery obtained as part of the Canadian Beaufort Sea program in the MacKenzie Delta area shows similar results to those obtained by Sellmann et al., (1975). Figure 15 represents two SLR images taken at 90° to each other showing the channels and lakes in the Delta. The dark areas in the main channel in Figure 15a represent high backscatter, meaning the channel is not frozen to the bottom as compared to the lighter areas which are (note that high backscatter is indicated by a dark image in Figure 15 and by a light image in Figure 16). Where the channel meanders, the ice on the shallow, inside portion of the meander freezes all the way to the bottom, whereas the outside of the curve where the water is much deeper, an ice-water interface exists. The thickness of the ice is of the order of 2 m. The high backscatter from the central part of the river does not vary very much since the incidence angle stays nearly constant. However, in Figure 15b, which shows part of the same portion of the channel the backscatter varies considerably as a function of incidence angle. This becomes even more pronounced if one compares the backscatter of the river with the one of the lakes

located at high incidence angles. It should also be noted that the large lake in Figure 15b shows variations in backscatter of the floating part of the ice cover which presently cannot be explained satisfactorily.

An operational application of SLR to fresh-water ice reconnaissance is shown in Figure 16. This imagery was obtained by the NASA Lewis Research Centre during February 1974 over the western end of Lake Superior as part of a demonstration program for the extension of the navigation season in the St. Lawrence River and the Great Lakes. Above the SLR image is an ice chart indicating the various ice types as interpreted from the radar image. It is interesting to note the large number of ship tracks extending from Two Harbours in the most direct line to the THIN-MED ice. Note that open water, which is indicated by the dashed lines in the bottom of the ice chart, cannot be distinguished in the SLR image from uniform thin ice in the Point Detour region. After processing of the SLR images and preparation of the interpretive chart, the composite was sent to a number of radio stations for transmission by radio link to vessels on the lakes.

Figure 17 shows a SLR image of the lower part of the Peterman glacier in north-west Greenland. Even though the glacier is covered with snow the lateral moraines are very distinct and can be traced to the tributary glaciers. There is also some evidence that the radar can detect subsurface

structures in this type of ice, although it would not be possible to establish this without extensive ground truth observations. Additional subsurface information can be obtained by using a 25 cm radar operating at near vertical incidence as reported by Elachi and Brown (1975).

Another area which shows great promise for the use of SLR is the detection and tracking of icebergs. Figure 18 taken off Cape Atholl near Thule, Greenland indicates a large number of icebergs which appear as light spots surrounded by darker first-year ice and open water. Here the light areas indicate high back scatter. Accurate counts of icebergs can readily be made. The minimum size of iceberg which can be detected is of the order of 10 m. The height of large icebergs could be obtained based on the length of the radar shadow. The movement of these kinds of icebergs could easily be monitored to determine if they will become potential hazards for offshore drilling in the Labrador Sea or shipping and fishing in the North Atlantic.

#### 3.4.2 Scatterometer

The microwave scatterometer is emerging as a powerful tool for determining ice type. The scatterometer is a calibrated down-looking airborne radar which can be used to measure the backscatter coefficient  $\sigma$ , as a function of aspect angle along a strip of terrain under an aircraft or spacecraft. Most scatterometers in existence today operate at roughly 13 GHz. Earlier work by Rouse (1969) and Parashar et al., (1975)

demonstrated the potential of scatterometry for use in determining different ice types. Recent, preliminary analysis of scatterometer data from the AIDJEX experiment has confirmed these earlier findings. In fact, the discrimination between first-year and multiyear ice is much greater than previously reported.

Figure 19 shows a photo mosaic of the test line A at the 1975 AIDJEX camp taken during April. The corresponding profiles from the dual-polarized 13.3 GHz scatterometer and the 37 GHz passive microwave radiometer have also been included. In this example the passive microwave radiometer was used to "ground truth" the scatterometer. As one can see there is an excellent correlation between the two sets of data. There is about a 60° difference in brightness temperature between first-year ice and multiyear ice and about 20 db difference in backscattering cross-section as observed by the scatterometer. The first broad plateau corresponds to the large lead identified earlier in the SLR image (Fig. 12). This is followed by multiyear ice and then by a small piece of first-year ice located just before the camp and another piece of first-year ice which constitutes the runway. The small first-year ice piece and the runway are clearly distinguishable in the SLR image (Fig. 12). The profile continues with a large segment of multiyear ice and ends with two small areas of first-year ice.

It can be seen from above that the SLR - Scatterometer combination forms a very powerful tool for use in determination

of sea ice type. The scatterometer is also a useful sensor in its own right for determining differences in ice type. The proposed scatterometer for SEASAT will undoubtedly yield useful information concerning ice type distribution on the mesoscale in the Arctic Ocean.

#### 3.4.3 Radar Altimeter

This sensor which is scheduled to be operated on SEASAT-A will determine the distance between the spacecraft and the ice-ocean surface to an rms precision of roughly  $\pm 10$  cm. The results are expected to be particularly useful in geodesy and in studies of significant wave heights. Inasmuch as the footprint of the radar is a 2 x 7 km spct, the results will not resolve individual roughness elements in the sea ice such as ridges and leads as is possible via an aircraft-borne laser profilometer. Nevertheless it may be possible to discern both spatial and temporal variations in the average (2 x 7 km) elevation of the surface of ice covered seas. These variations would presumably correlate with the intensity of ice deformation which has been shown to vary significantly between different provinces in the Arctic Ocean (Hibler, 1975). Other interesting studies that will be possible once SEASAT is launched concern the inter-relations between the results of the radar altimeter, the scatterometer, and the synthetic aperture radar.

#### 3.4.4 SAR (Synthetic Aperture Radar)

A number of countries (U.S.A., Canada, and countries of the European Space Agency) are carrying out programs with the aim of putting SAR's into space. The U.S. SEASAT-A program, the most advanced of these programs, is aimed at launching a SAR, complemented by a scatterometer radar altimeter, multifrequency microwave radiometer and a visible/IR radiometer in early 1978. Canada plans to put a SAR with complementary sensors (payload not defined yet) into space by spring 1984.

The SEASAT-SAR will operate in the L-band range and is expected to have a resolution as low as 25 m and a swath width of 200 km. At the present time the proposed circular orbit at an altitude of 800 km will allow SAR imagery to be obtained as far north as 77°N with repeat coverage every 36 hours.

If current orbit proposals are not altered, a large part of the Arctic Ocean will not be imaged by the SAR. It would be highly desirable to change the orbit enabling the SAR system to image well into the Arctic Ocean. It is very likely that future SEASAT-type missions will be launched into a polar orbit. For example, the Canadian POLESAT, as it may be named, is intended for a polar orbit.

The quality of the SAR imagery is expected to be similar to that of the L-band airborne SAR obtained by Ketchum and Tooma, (1973) and Elachi and Brown, (1975). Even though the resolution is higher than for X-band real aperture radars, the information content in the X-band imagery appears to be greater than for SAR

L-band. Because of the longer wavelength of the L-band SAR, the penetration (skin depth) is greater resulting in less scattering from the surface as compared with the X-band SLR. This is in accord with multifrequency passive microwave measurements made during AIDJEX 1975.

From the work accomplished so far and including the forthcoming results of the main AIDJEX experiment, some projections can be made of the kind of SAR product one may expect from SEASAT-A. Leads, ice boundaries as well as a variety of ice features such as ridges and rubble fields should be readily identifiable. Major ridging of first-year ice should be clearly seen, but multiyear ice ridges will not be as distinguishable. What would be difficult to determine are ice types, particularly the difference between first-year and multiyear ice. The successive tracking of the identifiable features will however permit quantitative information on ice drift and deformation to be obtained on an all-weather basis. We believe that the successful operation of the SEASAT SAR system will prove to be the first step in implementing an all-weather operational sea ice reconnaissance system that is useful to marine operators during the times of nearly continuous cloud that are encountered during the summer shipping season in the Arctic.

#### 4. SENSOR-ICE PHENOMENA COUPLING

##### 4.1 Distribution and Boundaries

Excellent pictures have been obtained from space showing the development and the dynamics of the boundaries between pack ice and the open ocean. For instance Figure 20, which was obtained by the SKYLAB astronauts over the northeastern part of the Gulf of St. Lawrence on January 11, 1974 (Campbell et al., 1975) shows a striking example of the ice plumes that occur to the east of Newfoundland and Labrador. The ice here is unconsolidated frazil which is kept from congealing by the continuous passage of waves through the plumes. These features appear to characteristically form at the edge of the pack during periods of high winds. The plumes can best be described as possessing a vortex type of structure. The small plumes that are composed of slush are elongated parallel to the surface wind. Figure 20b was taken on January 19 over the same general area. Again the most striking features off Newfoundland are the strongly developed plumes. Note the marked difference in the structure of these plumes compared to the ones on January 11, in that these plumes are elongated perpendicular to the surface wind direction as deduced from the stratocumulus bands. The earlier plumes were composed of slush, while this orientation change indicates that the present plumes are composed of small congealed pack ice floes with sizes below the resolution of the photograph.

A good example of the type of detailed information that is available, from a LANDSAT image on a clear day, on the distribution of open leads and thin ice areas within the pack is

shown in Figure 21. This image is interesting in that it contains a variety of thin ice as revealed by the varied grey tones in the image. This should be contrasted with the LANDSAT spring image shown in Figure 1(b) which only contains thick ice (> 1 m) and open water. Because of the striking albedo changes that are observed between open water or thin ice, and ice thicker than say 50 cm, the structure of open and newly refrozen leads can many times be observed through thin cloud layers.

Lead structure as obtained from a high resolution scanning microwave radiometer on board NASA's Convair 990 over the Bering Sea is shown in Figure 7 (Gloersen et al., 1974). The leads are located near the edge of the southerly advancing Bering Sea ice cover on February 20, 1973. The ice concentration is 84%. The boundary between the ice (grey ice) and the water is very distinct and sharp in this imagery. In many cases along the edges of the leads one can see thin blue lines. These lines indicate that the brightness temperature is lower due to the averaging effect of water and first-year ice within the beam of the antenna. This becomes very distinct in the ESMR imagery obtained from NIMBUS-5 shown in Figures 8 and 10.

From the previously presented examples of SLR imagery it is quite evident that often boundaries within the pack are very distinct, e.g. see the leads around the AIDJEX Big Bear shown in Figure 12. Unfortunately, in many cases it is not possible to distinguish open water from thin ice in ice infested waters. An

example of this is seen in Figure 18. The bottom centre of the SLR image represents open water and thin ice. The presence of open water was deduced due to the motion of the icebergs, determined from two SLR images taken at 20 min. intervals. If thin ice had been present, the icebergs would either have been stationary or two thin lines would have been visible due to the rough edge caused by the iceberg moving through thin ice. It should also be remembered that inasmuch as SLR primarily senses surface roughness as opposed to ice thickness, and that in principle thick undeformed first-year may be as flat as skim ice in a newly formed lead, the identification of newly formed leads in SLR imagery is to a considerable extent a matter of pattern recognition.

#### 4.2 Morphology

The ability to distinguish between open water, thin ice, first-year ice and multiyear ice is, of course, very important. For example both thickness and physical properties differ greatly between first-year and multiyear ice. Generally speaking first-year ice is smooth on the surface while the edges of first-year floes and ice fields are rather angular. In contrast, multiyear ice is generally rough on the surface while the edges of the floes are rounded. This change in the geometric characteristics of the ice is due to the fact that the melt which takes place during the summer modifies the surface, and also that the general "grinding" interaction between floes which with time tends to

round-off corners. These events are coupled with the formation of melt ponds and hummocks on the originally flat first-year ice surfaces. If this process is repeated over a number of years, the surface relief may become very pronounced.

Visual observations, aerial photography and to some extent SLR reveal these features permitting, for example, the preparation of maps which show the concentration of first-year and multiyear ice. As one can see, this is done more by circumstantial evidence rather than by direct observations of the material properties. The difficulty in distinguishing between such geometrical features increases depending on the amount of snow on the ice. A large amount of snow will often smooth out many of the surface features of multiyear ice making it difficult to distinguish multiyear from first-year ice.

IR scanners are not very useful in distinguishing thick first-year ice from multiyear ice. However, they can readily distinguish different varieties of thin ice, as well as, thin ice from thick ice (Gloersen et al., 1974).

Passive microwave radiometers, integrate the received electromagnetic radiation emitted from the surface over a relatively large area, therefore the resulting brightness temperature is generally independent of surface roughness.

The melt process during the summer not only modifies the surface features as mentioned earlier but also extensively changes the material properties themselves. Consequently the

dielectric properties of first-year and multiyear ice differ significantly and the distinction between these two important ice types using passive microwave radiometers becomes quite clear. Figures 5, 6, and 8 represent good examples of this capability.

The ability of SLR and passive microwave radiometers to penetrate snow in most cases eliminates the camouflaging effect snow has on ice.

In theory SLR should be as effective in distinguishing first from multiyear ice as shown by the results of the scatterometer in Figure 19. Unfortunately, the art of processing SLR signals obtained over ice has not progressed to the point which will permit this. In most cases, SLR imagery is still being used in a similar manner as aerial photography.

To obtain an idea of the distribution of surface roughness in the Arctic Ocean, Hibler (1975) has determined, by using laser profilometer data, some regional ridge height distributions. Figure 18 shows three height distributions for the Northern Canadian Archipelago, the area near the North Pole and the Beaufort Sea. The distributions indicate that the trend is from heavily to lightly ridged ice respectively. It is feasible that the altimeter on SEASAT-A may also give quantitative broad scale information on this subject.

#### 4.3 Thickness

Thickness of sea ice is probably the most important parameter for many transportation, engineering and climatological

applications. To date, there is no remote sensing instrument available which can directly measure the thickness of grey, first and multiyear ice. However, there are some promising developments in radar probes taking place (Bogorodskii and Tripol'nikov, 1974); Campbell and Orange, 1974; Chudobiak et al., 1974) which will be able to measure the time delay in an ice cover from which, combined with the dielectric constant, the thickness can be determined from a helicopter or a fixed wing aircraft.

As mentioned in the previous section IR techniques provide some possibilities for determining the thickness of thin ice up to 0.80 m depending on how cold the air temperature is (Gloersen et al., 1974).

SLR imagery can be used to infer ice thickness via the identification of ice types but such a method suffers for the reasons given in the morphology discussion.

On the other hand, passive microwave radiometers and scatterometers can identify ice types from which the thickness can then be inferred. The accuracy of the ensuing result depends on the sophistication of the assumed ice growth model. At best it can give a representative average value over a large area (Meeks, et al., 1974).

In the case of fresh water ice and glacier ice the situation is somewhat different. Operational systems are currently available which will measure directly the thickness of fresh

water ice. These have come to use primarily in the St. Lawrence Seaway and Great Lakes (Vickers et al., 1973; Chudobiak, et al., 1974; Page and Ramseier, 1975).

#### 4.4 Properties

Figure 23 illustrates a typical example of the salinity, density and temperature profiles of first and multiyear ice. In first-year ice the salinity is usually high both near the surface and at the bottom of the ice sheet. The density is nearly constant, except possibly near the upper surface where in some cases, it is lower. The temperature profile is generally linear during most of the year. In multiyear ice the salinity increases with depth, starting with a salinity of near zero in the ice that is above sea level. The density is also lower in the top part of multiyear ice covers. The temperature behaves in a similar fashion as in first-year ice. In addition, there appears to be a pronounced change in the internal structure of the upper (above water level) portions of sea ice that occurs during the first melt season. At this time the columnar, crystallographically oriented structure produced by initial crystal growth changes over to an equi-axed structure showing a random crystal orientation.

The dielectric properties also vary substantially from first-year to multiyear ice (Vant et al., 1974). Figure 24 summarizes the dielectric loss estimates obtained by a variety of investigators (Hoekstra and Cappillino, 1971; Bogorodskii and

Tripol'nikov, 1973; Vant et al., 1974 and Vant et al., 1975 to name a few). The dashed curve summarizes the preliminary results obtained during the 1975 spring AIDJEX program (Vant, personal discussion). These new results indicate that the losses in first-year ice are much less than previously believed. This is a significant result because it will aid in the interpretation of microwave signatures significantly and suggests that it should be possible to design radar probes that measure the sea ice thickness directly.

#### 4.5 Dynamics

Visible sensing systems such as LANDSAT have produced some highly useful results when applied over a large geographical area during an entire ice season (spring to fall) (Ramseier et al., 1974). However, the operational usefulness of such sensors is very restricted because of the limitations in daily coverage associated with the satellite orbit coupled with the cloud cover restriction. Passive and active microwave sensors on the other hand, are not limited by such restrictions and are capable of providing synoptic coverage. For instance, in Figure 6 a number of features can be traced over several days. The ice motion averages about 4 km a day to the west. The overall motions are complicated by the alternating anticyclonic-cyclonic activity over the area during this period (Campbell et al., 1975).

Due to the higher resolution of SLR imagery, similar but more detailed dynamic studies can be made. V.V. Bogorodskii and

V.S. Lohschilov (personal communication) have during the spring of 1973, made a SLR map of sea ice along the entire shipping lane north of the Eurasian continent. This map was made with the Toroz 16 GHz, real aperture system, and it appears that this system is now being used operationally for ship routing along the northern sea route. On-going studies using SLR imagery as part of the Canadian and USA continental shelf programs and AIDJEX are being pursued by the authors.

#### 4.6 Snow Cover

In most cases, snow cover acts as a camouflaging layer over the ice. The usefulness of visible sensors becomes very limited once the ice is covered by a snow cover. If the ice cover is not too thick, IR imagery is still useful in locating thin ice.

The advantage of active and passive microwave sensors lies in the fact that as long as the snow is dry, it is transparent to microwave radiation. All areas of thick ice shown in the SLR Figures 12-18 were snow covered. Similarly, the passive microwave images shown in Figure 5-8 and 10 had snow on the ice. For the amount of snow encountered in the Arctic, the effective emissivity is not much affected at the shorter wavelengths. Preliminary results obtained during AIDJEX 1975 indicate that vertically polarized microwave measurements are nearly independent of the amount of snowpack ( $-18^{\circ}\text{C}$ ) encountered as compared to horizontally polarized measurements which are strongly affected. The effect of liquid water in the snow on the

microwave emission from snow is striking. The emissivity at a wavelength of 8 mm increases from 0.78 to near unity as the liquid water content of the surface layer increases from 0 to 1% (Edgerton et al., 1971). These effects are similar in both the vertical and horizontal polarizations. As the liquid water content in snow on multiyear ice increases during the melt season the emissivity of the multiyear ice will approach the value for first-year ice. This has been observed in the ESMR images (Gloersen and Salomonson, 1975, Figure 19). However, this does not represent a serious problem inasmuch as ice type differences can easily be observed based on images taken during the dry snow period. However, it should be possible to map the progress of the melt season in the Arctic Ocean by studying microwave imagery.

## 5. SENSORS/TASK COUPLING

### 5.1 Research

The basic reason for acquiring remote sensing data on all forms of floating ice is to apply it to theoretical models so as to achieve a cause and effect understanding that will ultimately lead to a predictive capability. The models may be either highly elaborate numerical ones requiring frequent observations of numerous ice parameters or simple conceptual ones requiring occasional observations of one parameter.

In discussing models of floating ice, two scale distinctions are necessary. The time scale is of fundamental importance in

determining the types of sensor to be used in a given model. On a time scale basis, models can be divided into two types: dynamic models requiring observations on an hourly or daily basis and climate models requiring them on a weekly, monthly, or seasonal basis. The second scale distinction is the spatial scale. Small scale models, say of a given estuary or segment of coastline, require distinctly different sensor resolutions and areal coverage than do oceanic scale models.

#### 5.1.1 Ice Dynamics Models

Large scale dynamic ice models of pack ice, such as the AIDJEX model, require short time scale, high resolution images covering large spatial areas. Since the ice pack exists in regions of prolonged darkness and frequent cloud cover, the need for all-weather, day or night sensors is essential. In short, these sea ice models are the most demanding ones of all floating ice models in their remote sensing requirements. Therefore, all of the sensors discussed above have some applications to these models.

During periods of darkness or extensive cloud cover, the remote sensing needed as input to the dynamic models can be acquired by satellite-borne active and passive microwave sensors. The SAR would provide the high spatial resolution and synoptic sequential images necessary to map the ice velocity vector fields, the changing distribution of leads and polynyas and the variations in the edges of the pack. The passive microwave

sensors would provide data on the ice type, concentration, and divergence. Multifrequency passive microwave sensors can also provide, on an all-weather basis, data on surface snow accumulation rate, total snow amount, and the ice (not snow) surface temperature.

During periods of sunlight and minimal cloudiness, pack ice can be observed by visible and infrared sensors as well as by the microwave. Under these conditions, these sensors provide additional air/surface interface temperatures and the familiar visual ice signatures. The latter are invaluable because of the vast experience with visual observations by the community of ice scientists.

The same sensor coupling given above for sea ice applies as well to lake and river ice, with the important difference that the microwave sensors can be used to determine the thickness of the ice. Such observations are also less demanding on the observational system, since only mesoscale areas are involved.

Active microwave systems also appear to be the preferred sensors for acquiring data for dynamic models of ice shelves. Just as in the ice caps in which they originate, dynamic waves occur as a result of the flow produced by variations in mass balance. These waves have amplitudes ranging from several to tens of meters and wavelengths in the order of one to ten kilometers, easily resolvable by satellite-borne altimeters. Also, subsurface ice features can be observed with the satellite-

borne SAR. A key term in the mass balance of ice shelves is their calving rate, which could be accurately measured for the first time by using repetitive SAR observations.

#### 5.1.2 Climate Models

The full spectrum of remote sensing needs required by polar climate models is described in detail in the POLEX I and POLEX II reports published by the National Academy of Sciences, 1974. In this section, we wish to address the floating ice satellite observations pertaining to ocean-atmosphere interactions in the polar regions.

Climate models require ice remote sensing data that are both of lower spatial resolution and are obtained at larger time intervals than for ice dynamics models (see Table 1). The two primary forms of floating ice that relate to climatic variations are sea ice and shelf ice. Sea ice is a fundamental part of large-scale climatic processes because it undergoes great annual and seasonal variations in areal extent, its presence causes the significant alteration of the albedo of large oceanic areas, and it serves as an effective insulator in the ocean-atmosphere heat exchange. Ice shelves are also an important aspect of climate remote sensing, not because they are ordinarily prime movers in changes in climatic processes but because their variations are related to climatic change.

Because lower spatial resolutions are required for climate studies and because these data must be obtained on an all-weather

day or night basis, passive microwave sensors are again ideally suited. The frequency of coverage required by climate models is assured since ESMR and SMMR systems will be flown on satellites that are designed for more frequent observations for other purposes. In short satellite systems designed for acquiring data for floating ice dynamic models will collect, as part of their mission, all such data required by the climate models.

## 5.2 Operations

### 5.2.1 Transportation

Sea ice remote sensing from satellites has the capability of assisting surface shipping in ice-infested waters in two main classes of problems. The first of these is the problem of prediction of ice conditions for either the "long" - term or the "short" - term future. Here by "long" we mean 1 to 10 years in advance (information that might be used for planning) and by "short" we refer to 1 day to 2 weeks (useful in short term routing). The second problem is the one of specifying the ice conditions as they exist at any instant.

In long term prediction, rapid assessment of current conditions is not essential. Almost any sensor could conceivably be of use if it assists in either calibrating by measuring such parameters as the ice thickness distribution or in validating operational numerical models for ice drift and deformation. Therefore information collected by visual, IR and active and passive microwave sensors would be useful in providing

documentation on the state of the pack as a function of time. The exact parameters that would be measured from the imagery would, of course, depend upon the requirements of the specific model being used. These requirements would also change with time as the science of sea ice modeling changes. One important point about long term problems is that sensors that cannot penetrate clouds can still be extremely useful in that you always have enough time to have a day when conditions permit your favourite sensor to see the ice.

The problems of specifying the state of the ice at any instant in time and of short term forecasting are quite similar from a remote sensing point of view in that both require real-time or near real-time information. The ship captain needs to know where the line of least resistance is located in the vicinity of his ship. He cannot wait for a clear day to make his decisions. The same is true of operational short term forecasts; to predict the state of the ice tomorrow, you need to know its state today. The most promising sensor in this area is SAR which with its map-like format, ability to discern leads and highly deformed ice areas, its usefulness in studying ice drift and deformations and its all-weather capability make it extremely attractive. To be able to provide near real-time SAR processing and transmittal to ships is a large order that would, however, seem to be possible within the next few years. It should not be hard to convince maritime operators who are used to utilizing

ships radar of the utility of SAR imagery. Passive microwave imagery would also be useful but only if a significant increase in resolution can be achieved. The problems of rapid processing of microwave data are also severe.

#### 5.2.2 Coastal Engineering

The coastal engineering problem is rather different than the transportation problem in that it is primarily a design problem. As such one is more interested in extremes than in averages; what are the largest ice pile-ups, the highest drift rates, the thickest ice, the largest ice forces. Many of these problems cannot at present be addressed from satellites inasmuch as the items of interest (ice thickness, pressure ridge characteristics, ice strength) are either below the resolution of the sensor or simply cannot, as yet, be adequately measured remotely. Aircraft based systems such as laser profilometers, ice-thickness radar, and standard photography are, of course, very valuable. Satellite systems that would be of use are SAR which could provide valuable information on ice drift rates and deformation patterns and on the location of large areas of near coastal ridging and LANDSAT which would permit the determination of floe size distributions, the relative amount of brash ice that is present, and should when used in conjunction with SAR, assist in the identification of ice island fragments.

#### 5.2.3 Surveillance

Non-military surveillance is becoming increasingly important in areas of endeavour such as oil pollution control, and fisheries surveillance. This is due to the stepped up exploration of non-removeable resources offshore and in the arctic, and the strong interest coastal states are taking in managing a 200 mile economic limit, as proposed at the Law of the Sea conference. For example, Canada in 1972 passed the arctic waters Pollution Prevention Act which extends sovereignty (or control) 100 miles offshore above 60°N, half way between Greenland and Canada in the NE and along longitude 141°W.

To be able to control these zones established by national and international laws, all-weather remote sensing is required due to the large areas involved. These areas are for many coastal states located in ice infested water and regions which have predominantly a permanent ice cover for most of the year.

Another aspect concerns the surveillance of man's activity in remote areas. A good example is shown in Figure 13. A drill rig on an artificial island is located near the southern end of the SLR image. The regular pattern just west of the drill rig represent plowed trenches in the snow cover on top of shore fast ice. The dark lines south of the drill rig are plowed roads on ice, whereas the curved lines north of the rig are pressure ridges.

The type of sensors and systems required for such activities are of the type planned for SEASAT. It is envisaged that SAR

would provide the basic information with support of passive microwave radiometry.

#### 5.2.4 Biological Aspects

Ice infested oceans are, because of the logistical difficulties involved, places of meager biological observations. Yet in terms of biomass productivity the Bering Sea and the Antarctic Seas are among the most prolific areas on Earth. Remote sensing offers the only means to accurately assess the productivity of these regions and to monitor the populations of critical species. These observations are especially important now and in the next few years since many of the large sea animals, such as the mammals, are at the point of extinction due to oceanic pollution and over hunting.

Although most sea life can only be sensed indirectly by observing the way in which certain species affect their surroundings, such as the colour change of the sea surface due to plankton blooms, recent work shows that large sea mammals can be sensed directly (Ray and Wartzog, 1975). In the Bering Sea Mammal Experiment (BESMEX) walrus herds have been observed by airborne infrared images and their population estimated. In BESMEX the walrus is used as an indicator species, and by observing its distribution and relating its variations to sea ice dynamics it is hoped that the biological health of the walrus and other associated species can be monitored.

Whether or not sea mammals can be observed directly by satellite is yet to be seen. Shapiro and Burns (personal communication) are using LANDSAT imagery to map the distribution of various ice types in the Bering and Beaufort Seas that are associated with seals and walrus. By coupling these data with usual population estimates of these species from aircraft, it is hoped that accurate population estimates and migration patterns can be obtained.

Again the dynamics and morphology of sea ice must be observed on an all-weather, day or night basis if the techniques now being explored are to be made truly useful. Therefore high-resolution active microwave sensors may prove to have great potential in biological studies of animals associated with floating ice.

## 6. VIEW TO THE FUTURE

### 6.1 Future Ice Programs

#### 6.1.1 U.S.-Canadian Continental Shelf Ice Research

Both Canada and the U.S. are focusing a number of their research programs on the development of the natural resources of the arctic continental shelves and the arctic islands. In the U.S. the main current activity concerns itself with the NOAA (BLM) outer continental shelf arctic offshore program for the northern Bering Sea and the Chukchi Sea, while in Canada the Beaufort Sea program is terminating, the arctic islands pipeline

program has just commenced and a high arctic islands offshore program is on the drawing board.

It is clear that these programs should be concerned to a major extent with remote sensing from satellites. Unfortunately this is not the case. Instead, aircraft are being employed with a variety of sensors as a stop gap measure. When SLR is used it is in aircraft which have limited range or can fly only occasionally and at great cost. This kind of approach is very expensive and at the end does not provide the necessary data base for a comprehensive understanding of the environmental factors being sensed.

#### 6.1.2 Polex

The Polar Experiment (POLEX) is a polar research program for both hemispheres proposed by the Soviet Union (Treshnikov et al., 1968; Borisenkov and Treshnikov, 1971). The U.S. contribution to POLEX (National Academy of Sciences, 1974) discusses the experiment in detail. The objectives as defined for GARP (Global Atmospheric Research Program) of which POLEX is a part are twofold:

First GARP objective: An understanding of the transient behaviour of the atmosphere as manifested in the large-scale fluctuations that control changes of the weather; this would lead to increasing the accuracy of forecasting over periods from one day to several weeks.

Second GARP objective: An understanding of the factors that determine the statistical properties of the general circulation of the atmosphere, which would lead to better understanding of the physical basis of climate. In order to fulfill these objectives in the frame work of POLEX the POLEX panel recommends that maximum use be made of remote-sensing and unmanned data buoys. It recognizes also that some data is available from satellites, but no systematic analysis program exists that would be useful for climate studies. Furthermore, it does not seem practical to have long term observational programs based on manned stations. The emphasis should be towards creating a useful meteorological and oceanographic data set from satellite observations.

NIMBUS-G, SEASAT-A and its followers will be ideally suited for acquisition of the kind of information required to better understand the influence of polar regions on world climate.

#### 6.1.3 Nansen Drift Station

The Fridtjof Nansen Drift Station project proposes to freeze a decommissioned U.S. Coast Guard icebreaker into the ice pack of the Arctic Ocean at the edge of the continental shelf in the area north of the Lena Delta. The ship would then serve as a scientific platform as it drifts with the ice over the North Pole. It would then emerge from the pack after a time period of 2 to 3 years in the vicinity of Svalbard. Because the drift of the station will follow the general path of the Trans-Polar Drift

Stream, there will be a chance to observe the metamorphosis and dynamics of the ice as it changes from first to multiyear ice in the principal drift feature in the Arctic Ocean. Both satellite based and aircraft based remote sensing techniques will undoubtedly be useful in this program. Presumably radar ice thickness measurements, microwave and IR radiometer observations and laser profilometry would be performed from the helicopters based on the icebreaker. It might be possible to supplement these observations with SLR and microwave imagery obtained during the resupply flights. Finally an overview of the general ice area around the ship platform could be provided by LANDSAT and NOAA imagery. SAR measurements from SEASAT would also be extremely useful during the start and finish of the drift if the satellite orbit was changed so that imagery could be obtained up to 80°N. If the northern-most limit of SEASAT coverage remains at 75°N the Nansen drift track will almost completely be out of range. Even so the drift track is sufficiently far removed from standard satellite receiving stations that the sensor data will have to be recorded on "on board" tape recorders for later playback at a time that the satellite is over a receiving station. Inasmuch as the tape recorder capacity onboard most satellites is both limited and failure prone (if past satellites can be used as a guide), this may well prove to be the weak link in developing an adequate satellite program for the Drift Station.

#### 6.1.4 Operational Ice Forecasting

Operational ice forecasting is probably the most important and costly service governments provide to industry and agency operations. It has to be general and precise enough to be useful to a multitude of diverse users such as in marine operations, coastal engineering, and oil and gas industry to name a few. Current practise is to have ice observers on aircraft, who map the ice conditions by eye, aided in some cases by IR scanners, laser profilometers and search radars. These map include, besides open water and fast ice, four different concentration levels of ice for five different ice conditions such as thickness and floe size. There parameters, given above are the principal ones used in the Gulf of St. Lawrence and Bering Sea. The number of parameters increases considerably if one includes ice conditions in areas containing multiyear and fully developed first-year ice.

This requires the ice observer to be very judicial, and to have an exceptional ability for the synthesis and assimilation of synoptical information. The limited areal coverage severely reduces the general usefulness of this kind of operation except if a large number of aircraft and observers are at hand.

In order to optimize this type of operation to yield the economic benefits which have been identified by McQuillan and Clough (1975), and Nagler and McCandless, (1975) SEASAT must involve not only the acquisition of the necessary information, but also its reduction, analysis, the integration of various

sensor results, interpretation and the near real-time distribution of the final product. The format or formats of the final product should be designed in such a way to enable: the operator to use it in tactical situations; and the forecaster to use it for a series of short to long term forecasts. The climatologist requires the same type of information for his research.

## 6.2 The Ideal Operational Ice Satellite System

Increasing scientific and commercial interest in the remote sensing of floating ice indicates the need for operational satellite specifically designed for these purposes. It is clear that an operational satellite has to have an all-weather, day or night capability. Furthermore, to achieve the desired frequency of coverage and to image the areas of interest a number of satellites in a polar orbit will be required.

In order to achieve the required high resolution imagery it will be absolutely necessary to utilize active microwave systems. The current contemplated L-band SAR for SEASAT-A may not give all the necessary details required but possibly in conjunction with an added X-band frequency system could provide a complete data set. A multifrequency passive microwave scanner of higher resolution than the current SMMR planned for NIMBUS-G and SEASAT-A is another basic requirement for an operational satellite.

Combining the data products of MSAR (Multifrequency

Synthetic Aperture Radar) with SMMR would provide the necessary basic information for an operational ice satellite.

As pointed out earlier the methods and procedures employed to get the information in an integrated form to the user is a formidable task in itself. The basic requirement is to have near-real time imagery in the users hand, at great distances from the receiving station, within a few hours of obtaining it. This will require the transmission of the various sensor data to some sort of command and control centre (Morley and Clough, 1975) where the reduction, analysis, integration and interpretation takes place. The final product should go via communication satellite, or in some cases over telephone lines, back to the user. If the final product is an image it has to be of very high quality at a price the user can afford.

It is encouraging to note that some progress is being made in the implementation of similar information systems. This progress may prove very beneficial to the planners of the future operational satellite systems. For example Shaw (1975) and Gedney et al., (1975) have shown that near-real time transmission of satellite imagery and real-time transmission of SLR imagery respectively, can be accomplished successfully with a resulting high quality user product.

Finally the proposed SEASAT-A satellite scheduled for launch in April 1978 will provide an excellent data base for the type of information required in an operational ice satellite system. It

is hoped that international cooperation will prevail in putting an operational SEASAT-type system together.

7. ACKNOWLEDGEMENT

R.O. Ramseier would like to acknowledge the support of the Polar Continental Shelf Project, the Department of National Defence and the Canadian Centre for Remote Sensing. W.F. Weeks would like to acknowledge the support of the Arctic Programs, Office of Naval Research.

8. REFERENCES

- Ackley, S.F., and Hibler, W.D. (1975). Measurements of Arctic Ocean ice deformation and fracture patterns from satellite imagery. In "SCOR/SCAR Polar Oceans Conference, Montreal, May 1974 (M. Dunbar, ed.)", Cambridge, Scott Polar Research Institute.
- Barnes, J.C., Chang, D.T., and Willand, J.H. (1972). Application of ITOS and NIMBUS infrared measurements to mapping sea ice. Final Report Contract No. 1-36025 to NOAA (NESS) by Allied Research Associates, 87 pp.
- Barnes, J.C., and Bowley, C.J. (1974). The application of ERTS imagery to monitoring Arctic sea ice. Lexington, Mass., Environmental Research and Technology, Inc. (ERT Document 0408-F).
- Barnes, J.C., and Bowley, C.J., and Smallwood, M.D. (1975). The application of imagery to monitoring Arctic sea ice: Supplemental Report. Lexington, Mass., Environmental Research and Technology, Inc. (ERT Document 0408-S).
- Bogorodskii, V.V., and Tripol'nikov, V.P. (1973). Electro magnetic characteristics of sea ice in the range of 30-400 MHz. Akademiga Nauk SSSR Doklady, 213, p. 577-579.
- Bogorodskii, V.V., and Tripol'nikov, V.P. (1974). Radar sounding of sea ice. Zhurnal Tekhnicheskoy Fiziki 44(3), p. 660-662.
- Borisenkov, E.P., and Treshnikov, A.F. (1971). On the role of polar regions in the problem of the global investigation of the circulation of the atmosphere and ocean. Trudy of the Arctic and Antarctic Institute, 296, Leningrad.
- Campbell, W.J., and Orange A.S. (1974). A continuous profile of sea ice and freshwater ice thickness by impulse radar. Polar Record 17(106), p. 31-41.
- Campbell, W.J., Gloersen, P., Nordberg, W., and Wilheit, W.W. (1974). Dynamics and morphology of Beaufort Sea ice determined from satellites, aircraft, and drifting stations. In "Symposium on Approaches to Earth Sciences through Use of Space Technology" (P. Bock, ed.), Konstanz, Federal Republic of Germany (23-25 May 1973), p. 311-27, Akademie-Verlag.
- Campbell, W.J., Weeks, W.F., Ramseier, R.O., and Gloersen, P. (1975). Geophysical studies of floating ice by remote sensing. Journal of Glaciology 15 (73).

- Campbell, W.J., Ramseier, R.O., Weeks, W.F., and Wayenberg, J.A. (1975). Visual observation of floating ice from SKYLAB. SKYLAB Visual Observation Project Rept. No. 2, Johnson Space Center, Houston, Texas.
- Campbell, W.J., Gloersen, P., Ramseier, R.O., Webster, W.J., and Wilheit, T.T. (in press) Beaufort Sea ice zones by means of microwave imagery. Journal of Geophysical Research.
- Chang, T.C., Gloersen, P., Schmuggs, T., Wilheit, T.T., and Zwally, H.J. (1975). Microwave emission from glacier ice, NASA - Goddard Space Flight Center, Greenbelt, Maryland. Preprint X-910-75-36.
- Chase, P. (1972). Using ITOS vidicon and scanning radiometric data for Great Lakes ice analysis and prediction. NOAA/NESS Contract 1-36012, The Bendix Corporation, Aerospace Systems Division, Ann Arbor, MI.
- Chudobiak, W.J., Gray, R.B., Ramseier, R.O., Makios, V., Vant, M., Davies, J.L., and Katsube, J. (1974). Radar remote sensors for ice thickness and soil moisture measurements. Proceedings Second Canadian Symposium on Remote Sensing, (Guelph, Ontario), p. 418-424.
- DeRycke, R.J. (1973). Sea ice motions off Antarctica in the vicinity of the eastern Ross Sea as observed by satellite. Journal of Geophysical Research 73(36), 8873-8879.
- Dickinson, L.J., Boselly, S.E., and Burgmann, W.S. (1974). Defense Meteorological Satellite Program (DMSP) Users' Guide. Air Weather Service (MAC), United States Air Force AWS TR-74-250, Hq, AWS, Scott AFB, Illinois 62225, 109 pp.
- Dunbar, M., and Wittmann, W. (1963). Some features of ice movement in the Arctic Basin. In "Proceedings Arctic Basin Symposium (Hershey, Pennsylvania, October 1962), p. 90-104, Arctic Institute of North America.
- Dunbar, M., and Weeks, W.F. (1975). The interpretation of young ice forms in the Gulf of St. Lawrence using side looking airborne radar and infrared imagery. Cold Regions Research and Engineering Laboratory Research Report 337, 41 pp.
- Edgerton, A.T., Stogryn, A., and Poe, G. (1971). Microwave radiometric investigations of snow pack. Final Report No. 1285R-4 for U.S.G.S. contract no. 1A-08-001-11828, Aerojet-General Corporation Microwave Division, El Monte, California.

- Elachi, J., and Brown, W.E., Jr., (1975). Imaging and soundings of ice fields with airborne coherent radars. *Journal of Geophysical Research* 80(8), p. 1113-1119.
- Gedney, R.T., Schertler, R.J., Mueller, R., Jirberg, R.J., and Mark, H., (1975). An operational all-weather Great Lakes ice information system. *Proceedings, Third Canadian Remote Sensing Meeting, Edmonton, Alberta.*
- Gloersen, P., Nordberg, W., Schmuggs, T.J., Wilheit, T.T., and Campbell, W.J. (1973). Microwave signatures of first-year and multiyear sea ice. *Journal of Geophysical Research* 78(18), p. 3564-72.
- Gloersen, P., Chang, T.C., Wilheit, T.T., and Campbell, W.J. (1974). Polar sea ice observations by means of microwave radiometry. *Proceedings Inter-disciplinary Symposium on Advanced Concepts and Techniques in the Study of Ice and Snow Resources, Monterey, California, p. 541-550, National Academy of Science.*
- Gloersen, P., Ramseier, R.O., Campbell, W.J., Chang, T.C., and Wilheit, T.T. (1974). Variation of the morphology of selected micro-scale test areas during the Bering Sea Experiment. In "Results of the U.S. Contribution to the joint U.S./U.S.S.R. Bering Sea Experiment". Greenbelt, Maryland, Goddard Space Flight Center, p. 104-21. (NASA X-910-74-141).
- Gloersen, P., Ramseier, R.O., Campbell, W.J., Kuhn, P.M., and Webster, W.J., Jr. (1974). Ice thickness distribution as inferred from infrared and microwave remote sensing during the Bering Sea Experiment. In "Results of the U.S. Contribution to the joint U.S./U.S.S.R. Bering Sea Experiment". Greenbelt, Maryland, Goddard Space Flight Center, p. 104-21. (NASA X-910-74-141).
- Gloersen, P., and Salomonson, V.V. (1975). Satellites - New global observing techniques for ice and snow. *Journal of Glaciology*, 15(73).
- Hibler, W.D., Ackley, S.F., Crowder, W.K., McKim, H.L., and Anderson, D.M. (1974). Analysis of shear zone ice deformation in the Beaufort Sea using satellite imagery. In "The Coast and Shelf of the Beaufort Sea", (J.C. Reed and J.E. Sater, eds.), Arlington, Virginia, p. 285-296 Arctic Institute of North America.

- Hibler, W.D., Tucker, W.B., and Weeks, W.F. (1975). Techniques for studying sea ice drift and deformation at sites far from land using LANDSAT imagery. Proceedings of the 10th International Symposium on Remote Sensing of Environment, 1975 Ann Arbor. Willow Run Laboratories, Environmental Research Institute of Michigan.
- Hibler, W.D. (1975). Characterization of cold regions terrain using airborne laser profilometry. *Journal of Glaciology* 15(73).
- Hoekstra, P., and Capillino, P. (1971). Dielectric properties of sea and sodium chloride ice at UHF and microwave frequencies. *Journal of Geophysical Research*, 76(20), p. 4922-4931.
- Ketchum, R.D., Jr., and Tooma, S.G., Jr. (1973). Analysis and interpretation of airborne multi-frequency - Side Looking Radar sea ice imagery. *Journal of Geophysical Research*, 78(3) p. 520-538.
- McClain, E.P. (1974a). Earth satellite measurements as related to sea ice studies. In "COSPAR Symposium on Approaches to Earth Survey Problems Through Use of Space Techniques, Constance, F.R.G., May 1973" (P. Bock, ed.), Akademie-Verlag, Berlin.
- McClain, E.P. (1974b). Some new satellite measurements and their application to sea ice analysis in the Arctic and Antarctic. In "Advanced Concepts and Techniques in the Study of Snow and Ice Resources" (H.S. Santeford and J.L. Smith, eds.), Washington, National Academy of Sciences, p. 457-466.
- McQuillan, A.K., and Clough, D.J. (1975). Benefits of remote sensing systems to petroleum operations in Canadian ice infested waters. Proceedings, Third Symposium on Remote Sensing, Edmonton, Alberta.
- Meeks, D.C., Ramseier, R.O., and Campbell, W.J. (1974). A study of microwave emission properties of sea ice - AIDJEX 1972. Proceedings Ninth International Symposium on Remote Sensing of Environment, University of Michigan, Ann Arbor.
- Morely, L.W., and Clough, D.J. (1975). Proposal for an arctic operations centre. Proceedings, Third Canadian Symposium on Remote Sensing, Edmonton, Alberta.
- Nagler, R.G., and McCandless, S.W. (1975). Operational Oceanographic Satellite - SEASAT potential for oceanography, climatology, coastal processes and ice. NASA - Headquarters, Washington, D.C. (draft report).

- National Academy of Sciences, (1974). U.S. contribution to the Polar Experiment (POLEX). Part 1 POLEX-GARP (North); and Southern Ocean Dynamics, a strategy for Scientific Exploration 1973-1983.
- Nye, J.F. (1975). The use of ERTS photographs to measure the movement and deformation of sea ice. *Journal of Glaciology* 15(73).
- Page, D.F., and Ramseier, R.O. (1975). Application of active radar techniques to the study of ice and snow. *Journal of Glaciology* 15(73).
- Parashar, S.K., Biggs, A.W., Fung, A.K., and Moore, R.K. (1975). Investigation of radar discrimination of sea ice. Proceedings of the Ninth Symposium on Remote Sensing of Environment, University of Michigan, Ann Arbor.
- Poulin, A.O. (1973). On the thermal nature and sensing of snow-covered Arctic terrain. U.S. Army Topographic Laboratories Research Note ETL-RN-73-4, 173 pp.
- Poulin, A.O. (1975). Significance of surface temperature in the thermal infrared sensing of sea and lake ice. *Journal of Glaciology* 15(73).
- Ramseier, R.O., Campbell, W.J., Weeks, W.F., Arsenault, L.D., and Wilson, K.L. (1974). Ice dynamics in the Canadian Archipelago and adjacent Arctic Basin as determined by ERTS-1 observations. International Symposium on Canada's Continental Margins and Offshore Petroleum Exploration, Calgary 1974.
- Ramseier, R.O., Gloersen, P., and Campbell, W.J. (1974). Variation in the microwave emissivity of sea ice in the Beaufort and Bering Sea. In "Specialist Meeting on Microwave Scattering and Emission from the Earth (E. Schanda, ed.)", Proceedings of the URSI, Commission II, p. 87-93, Institute of Applied Physics, University of Bern, Switzerland.
- Ramseier, R.O., Campbell, W.J., Weeks, W.F., Arsenault, L.D., and Wilson, K.L. (1975). Ice dynamics in the Canadian Archipelago and adjacent Arctic Basin as determined by ERTS-1 observations. In "International Symposium on Canada's Continental Margins and Offshore Petroleum Exploration (Calgary, Sept. 1974)," Canadian Society of Petroleum Geologists.
- Rothrock, D.A., and Hall, R.T. (1975). Testing the redistribution of sea ice thickness from ERTS photographs. AIDJEX Bulletin No. 29 p. 1-19.

- Rouse, J.W., Jr. (1969). Arctic ice type identification by radar. Proceedings of the IEEE, 57(4), p. 605-611.
- Sellmann, P., Weeks, W.F., and Campbell, W.J. (1975). Use of side-looking airborne radar to determine lake depth on the Alaskan North Slope. Cold Regions Research and Engineering Laboratory Special Report 230, 6 pp.
- Shaw, E. (1975). Near real-time transmission of sea ice satellite imagery. Proceedings, Third Canadian Symposium on Remote Sensing, Edmonton, Alberta.
- Streten, N.A. (1974). Large-scale sea ice features in the western Arctic Basin and the Bering Sea as viewed by the NOAA-2 satellite. Arctic and Alpine Research 6(4), p. 333-345.
- Swithinbank, C.W.M., and Zumberge, J.H. (1965). The ice shelves. In "Antarctica (T. Hatherton, ed.)", London Methuen and Co. Ltd., p. 199-220.
- Swithinbank, C.W.M. (1972). Arctic pack ice from below. In "Sea Ice, Proceedings of an International Conference (T. Karlsson, ed.)", p. 246-254. National Research Council, Reykjavik, 1972).
- Thorndike, A.S., Rothrock, D.A., Maykut, G.A. and Colony, R. (1975). The thickness distribution of sea ice. Journal of Geophysical Research.
- Treshnikov, A.F., Borisenkov, Ye.P., Nikiforov, E.G., Mustafin, N.V., Chaplygin, E.D., and Shpaikher, A.O. (1968). An ocean-atmosphere interaction experiment for the Arctic. Probl. Arkt. Antarkt. No. 28. Translated by the RAND Corporation, November 1969.
- Vant, M.R. Gray, R.B., Ramseier, R.O., and Makios, V. (1974). Dielectric properties of fresh and sea ice at 10 GHz. Journal of Applied Physics, 45(11) p. 4712-4717 and 46(5) p. 2339 (1975).
- Vickers, R.S., Heighway, J., and Gedney, R. (1973). Airborne profiling of ice thickness using a short pulse radar. In "Advanced Concepts and Techniques in the Study of Snow and Ice Resources", (H.S. Santeford and J.L. Smith, eds.). National Academy of Sciences, p. 422-431.
- Weeks, W.F., and Assur, A. (1969). Fracture of lake and sea ice. Cold Regions Research and Engineering Laboratory Research Report 269, p. 77.

- Weeks, W.F., Kovacs, A., and Hibler, W.D. (1971). Pressure ridge characteristics in the Arctic coastal environment. In "Proceedings First International Conference on Port and Ocean Engineering under Arctic Conditions, 23-30 August 1971", Vol. I, p. 152-183, Department of Port and Ocean Engineering, Technical University of Norway, Trondheim.
- Weeks, W.F. and Campbell, W.J. (1973). Icebergs as a fresh water source: an appraisal. *Journal of Glaciology* 12(65), p. 207-233.
- Weeks, W.F. and Campbell, W.J. (1975). The remote sensing plan for the AIDJEX main experiment. *AIDJEX Bulletin* No. 29, p. 21-48.
- Wilheit, T.T., Nordberg, W., Blinn, J., Campbell, W.J., and Edgerton, A. (1972). Aircraft measurements of microwave emission from Arctic sea ice. *Remote Sensing of Environment* 2(3), p. 129-139.

9. FIGURE CAPTIONS

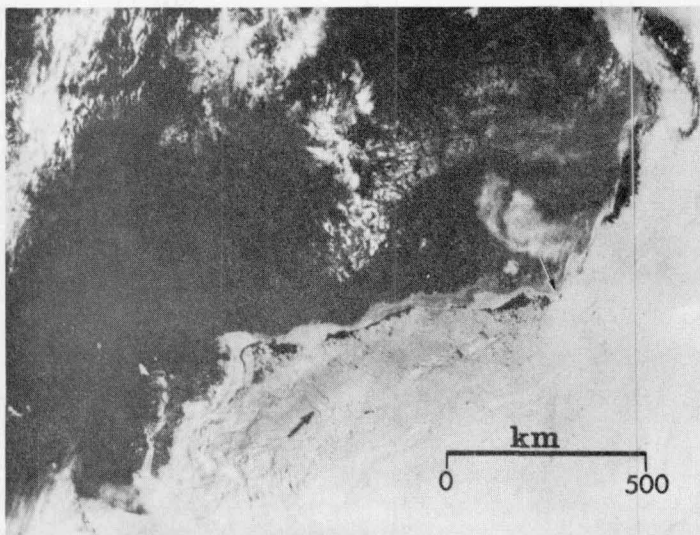
1. NOAA, LANDSAT and U-2 imagery obtained over the same ice area in the Beaufort Sea at essentially the same time on 21 June 1974:
  - (a) NOAA VHRR image, the arrow on the left points to Barrow, Alaska; the arrow on the right points to a large lead that is also visible in (b). Careful examination reveals many ice features, (floes and leads) that are also visible in the LANDSAT image;
  - (b) LANDSAT image from the Beaufort Sea north of Barter Island, Alaska; the arrow on the right indicates a large lead visible in the NOAA image (a) while the arrow on the left indicates an unusual shaped "branching" lead that is visible in the U-2 photograph (c). The LANDSAT image is 185 km on a side;
  - (c) U-2 photograph of the Beaufort Sea north of Barter Island, Alaska; the arrow indicates a lead that is also visible in the LANDSAT image but not in the NOAA image. Flight elevation was 20,000 m.
2. Sonar profile of the underside of the Arctic pack ice obtained from H.M.S. Dreadnought during its North Pole cruise in March 1971: both profiles show the ice canopy at 83 N, 06 E (Swithinbank, 1972).
3. DMSP image of Northern Alaska on 22 April 1975 (with Barrow indicated by the arrow) and the Arctic Ocean. The lead patterns which were only poorly visible on the normal VHR image were enhanced by spreading the 16 grey shades over a 25 K temperature interval bounded on the upper end by the freezing temperature of sea water.
4. IR image of CSS Dawson travelling south through the ice in the Gulf of St. Lawrence during January 1974. The warmest temperatures (black) are given by the open water and the ships smoke-stack. The thickest ice (white) was approximately 40 cm (Dunbar and Weeks, 1975).
5. False-colour ESMR image ( $\lambda = 1.55$  cm) collected on the NASA CV-990 aircraft over the AIDJEX areas, Beaufort Sea:
  - (a) Mosaic obtained on 15 March 1971 from 11 km altitude with image centred at about  $74^{\circ} 6'N$ ,  $131^{\circ} 17'W$ . The AIDJEX campsite is within the circle.
  - (b) Mosaic obtained on 12 April 1972 from 11 km altitude with image centred at about  $75^{\circ}N$ ,  $150^{\circ}W$ . The AIDJEX camp is within the circle at the bottom of the image.

6. Successive false-colour ESMR image strips collected between 4 and 23 April 1972 of sea ice of the western Beaufort Sea from Harrison Bay, Alaska to 74°N.
7. False-colour ESMR image collected on 20 February 1973 on NASA CV-990 aircraft over the BESEX area, Bering Sea. The image is centred near 61° 24'N, 176° 24'W.
8. False-colour ESMR mosaics collected over the northern hemisphere on 11 January 1973 and 8 September 1973 depicting seasonal changes in the Arctic sea ice canopy.
9. Seasonal variations of sea ice in the northern hemisphere.
10. False-colour ESMR mosaics collected over the southern hemisphere on 15 December 1972 and 26 February 1973 depicting seasonal changes in the Antarctic Sea ice canopy.
11. Seasonal variations of sea ice in the southern hemisphere.
12. SLR image of AIDJEX area taken by DND Argus Aircraft with a Motorola AN/APS 94D real aperture radar during April 1975. The dark spot in the centre of the image is the AIDJEX camp "Big Bear". Light areas indicate low returns and dark areas indicate high returns. Image was taken by the port antenna with the aircraft flying in a northerly direction.
13. SLR image of McKenzie Delta area taken by the DND Argus Aircraft with a Motorola AN/APS 94D real aperture radar during April 1975. Image was taken by the port antenna with the aircraft flying in a northerly direction. Light areas indicate low return and dark areas high returns. Note the man-made disturbances of the snow cover on the shore fast ice at the beginning of the image. Black lines across the image are time reference marks.
14. SLR image of the western part of Lake Superior taken by a Mohawk aircraft with the Motorola AN/APS 94C real aperture radar on 6 February 1974. The dark areas indicate low returns and the light areas indicate high returns (Vickers et al., 1973).
15. SLR image of area just west of Harrison Bay, Alaska taken by a U.S.G.S. Mohawk aircraft with a Motorola AN/APS 94XE1 real aperture radar during April 1974. The image includes Naluakruk, Okalik and part of Teshekpuk Lakes. Note the differences in radar return from lakes which at the time the image was made were covered with 2 m of ice (Sellmann et al., 1975).

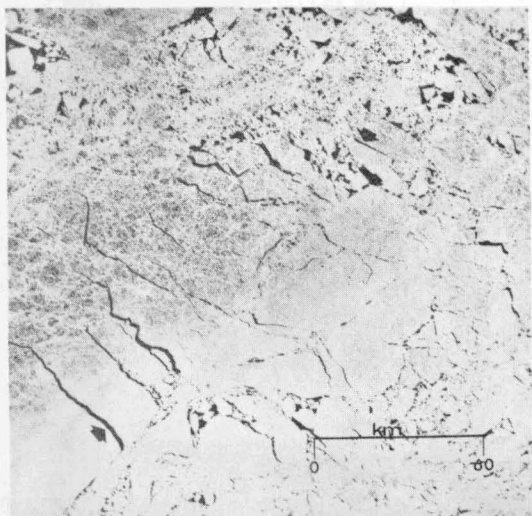
16. SLR image with McKenzie Delta channels and lakes taken by the DND Argus aircraft with a Motorola AN/APS 94D real aperture radar on April 1975. Image was taken by the port antenna which was used to image the main channel twice at 90 to each other. The light areas indicate low returns and the dark areas indicate high returns.
17. SLR image of Peterman Glacier, northwest Greenland taken by the DND Argus aircraft with a Motorola AN/APS 94D real aperture radar on March 1975. Dark areas indicate high returns and light areas low returns. The aircraft was flying in an easterly direction.
18. SLR image of icebergs off the coast of Cape Atholl, near Thule, Greenland taken by the DND Argus aircraft with a Motorola AN/APS 94D real aperture radar on March 1975. Dark areas indicate low returns and light areas high returns. The image was taken by the port antenna while the aircraft was flying in a southerly direction.
19. Photo mosaic, scatterometer and passive microwave radiometer profiles of line A taken by CCRS C-47 aircraft over the AIDJEX camp area during April 1975. The polarization for the 13.3 GHz scatterometer is in the HV mode and the increase in scattering is plotted downward. The vertical polarized profile of the 37 GHz passive microwave radiometer (Aerojet Electrosystems) is plotted with increasing brightness temperature upwards. Note the plateau areas of the microwave data taken at 45 forward corresponding to the lead at the beginning and the first-year ice at the end of the photo mosaic.
20. SKYLAB-4 images taken by the astronauts over the Gulf of St. Lawrence -
  - (a) 11 January 1974, NE part of Gulf of St. Lawrence, Straits of Belle Isle. Note the frazil ice plumes parallel to the wind direction.
  - (b) 1 January 1974, NE part of Gulf of St. Lawrence, Straits of Belle Isle. Note the consolidated ice pack and ice plumes perpendicular to the wind direction.
21. LANDSAT (MSS-7) image of pack ice in the central Beaufort Sea ( $77^{\circ} 52'N$ ,  $138^{\circ} 04'W$ , 30 March 1975). The image is 185 km on a side.
22. Ridge height distributions taken in February 1973. Each distribution was taken from a laser track approximately 40 km in length and the average number of ridges per kilometer above 4 ft (1.22 m) is denoted by  $\mu$  for each distribution. The two-parameter fit is indicated by dashed lines with the

actual data being solid. Distribution a, was observed at approximately lat.  $83^{\circ}$ N., long.  $85^{\circ}$ W., b at lat.  $87^{\circ}$ N., long.  $162^{\circ}$ W., c at lat.  $70^{\circ}$ N., long.  $139^{\circ}$ W. The mean ridge heights for distributions a, b and c were 1.93 m, 1.70 m, and 1.57 m respectively (Hibler, 1975).

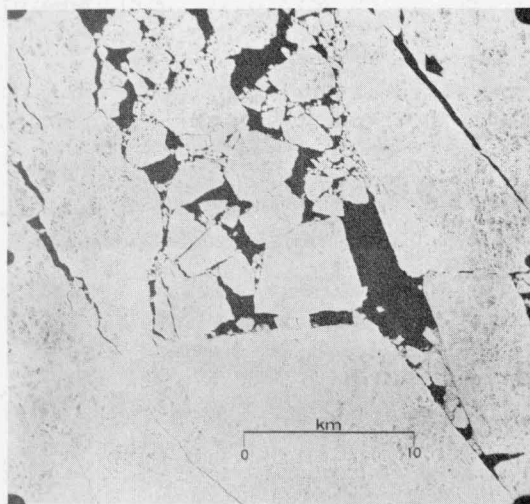
23. Depth profiles of salinity, density and temperature for first-year and multiyear ice obtained during April 1975 at the AIDJEX camp. The schematic of the core is shown on the left hand side of the profiles indicating the structural changes in the ice cover.
24. Summary of the dielectric loss data for ice of a standard salinity and of a standard temperature. The dashed line indicates the trend of the 1975 AIDJEX results obtained by Vant (personal communication).



(a) NOAA VHRR image, the arrow on the left points to a large lead that is also visible in (b). Careful examination reveals many ice features, (floes and leads) that are also visible in the LANDSAT image.



(b) LANDSAT image from the Beaufort Sea north of Barter Island, Alaska; the arrow on the right indicates a large lead visible in the NOAA image (a) while the arrow on the left indicates an unusual shaped "branching" lead that is visible in the U-2 photograph (c). The LANDSAT image is 185 km on a side.



(c) U-2 photograph of the Beaufort Sea north of Barter Island, Alaska; the arrow on the right indicates a large lead that is also visible in the LANDSAT image but not in the NOAA image. Flight elevation was 20,000 m.

FIGURE 1. NOAA, LANDSAT and U-2 imagery obtained over the same ice area in the Beaufort Sea at essentially the same time on 21 June 1974.

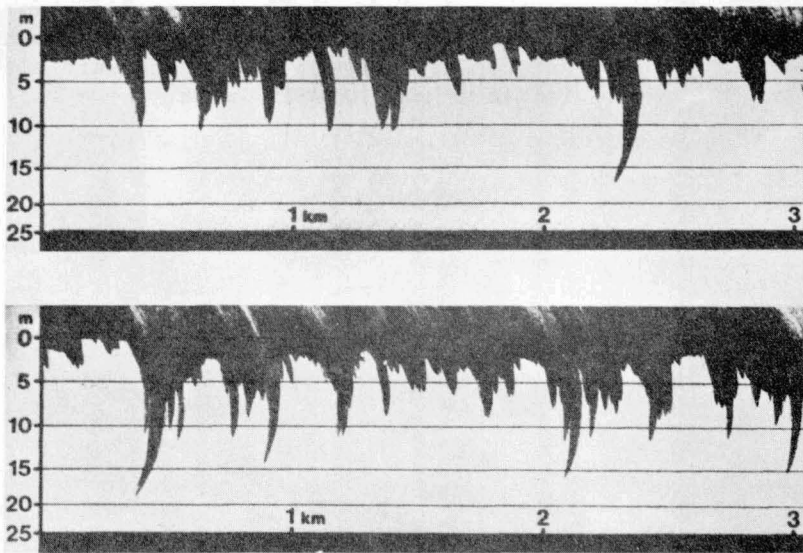


FIGURE 2. Sonar profile of the underside of the Arctic pack ice obtained from H.M.S. Dreadnought during the North Pole cruise in March 1971: both profiles show the ice canopy at  $83^{\circ}\text{N}$ ,  $06^{\circ}\text{E}$  (Swithinbank, 1972).

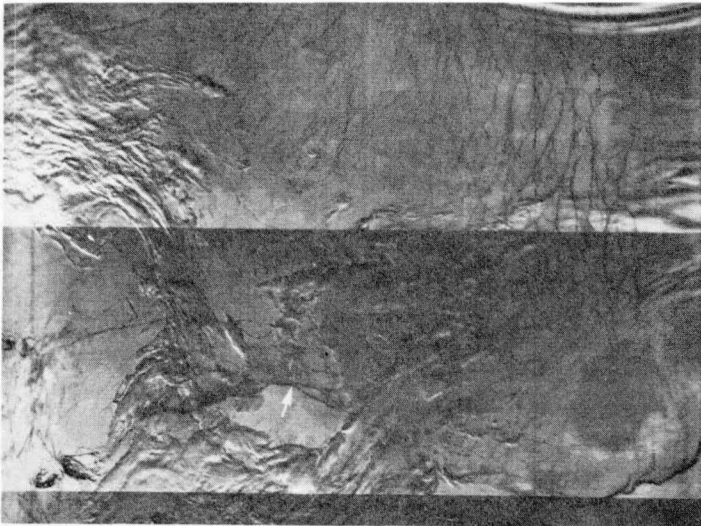


FIGURE 3. DMSP image of Northern Alaska on 22 April 1975 (with Barrow indicated by the arrow) and the Arctic Ocean. The lead patterns which were only poorly visible on the normal VHR image were enhanced by spreading the 16 grey shades over a  $25^{\circ}\text{K}$  temperature interval bounded on the upper end by the freezing temperature of sea water.

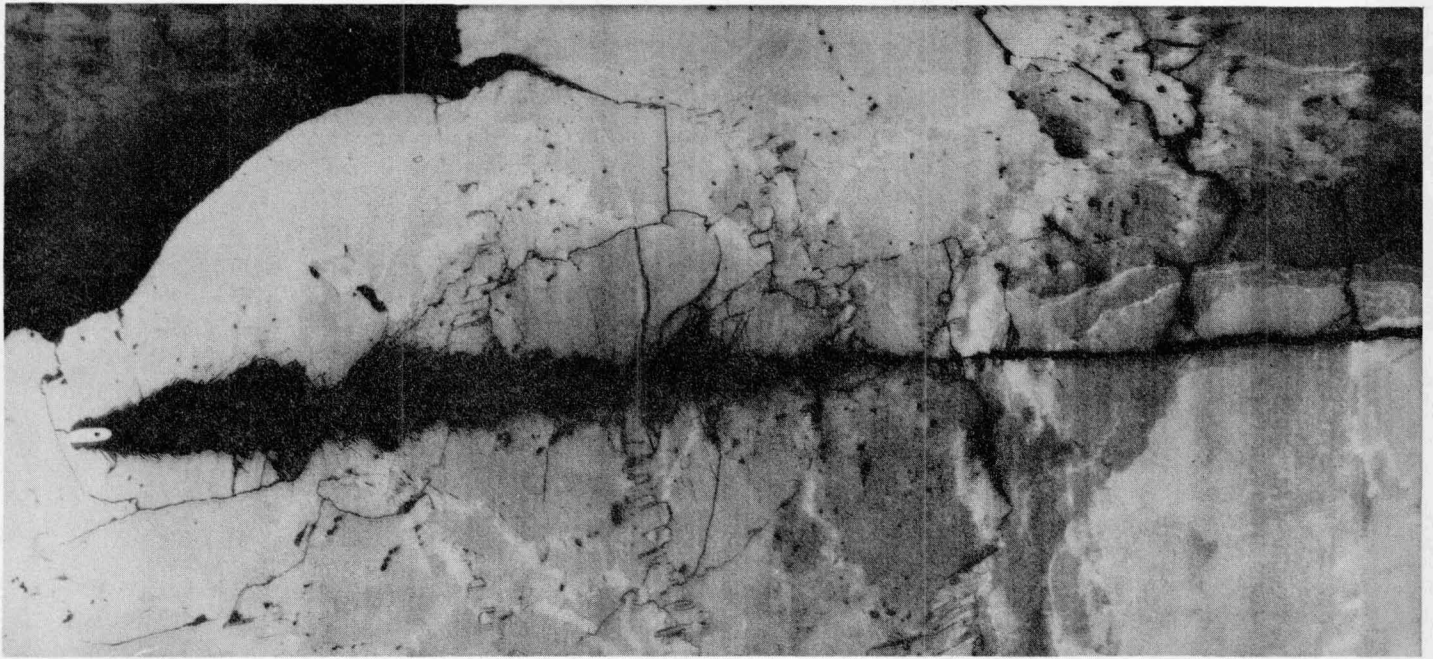


FIGURE 4. IR image of CSS Dawson travelling south through the ice in the Gulf of St. Lawrence during January 1974. The warmest temperatures (black) are given by the open water and the ships smoke-stack. The thickest ice (white) was approximately 40 cm (Dunbar and Weeks, 1975).

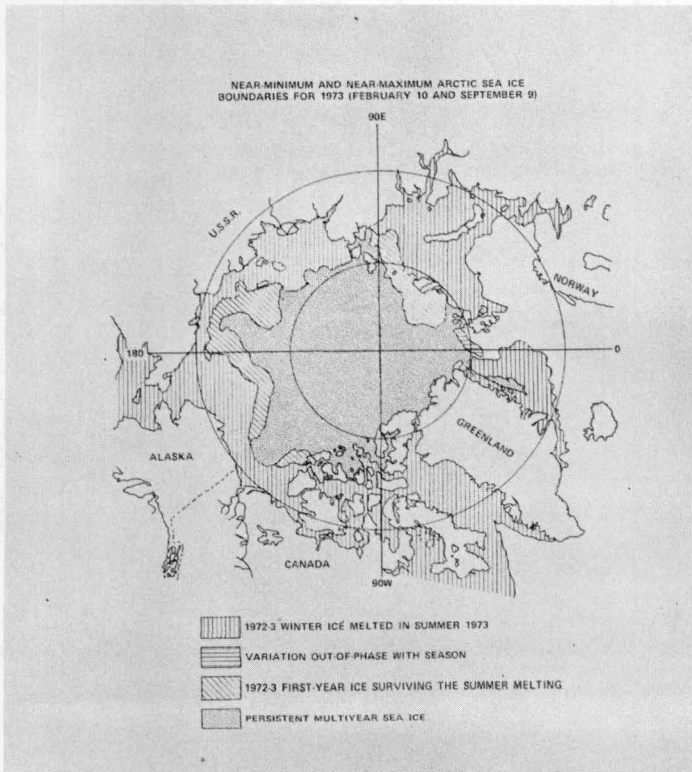


FIGURE 9. Seasonal variations of sea ice in the northern hemisphere.

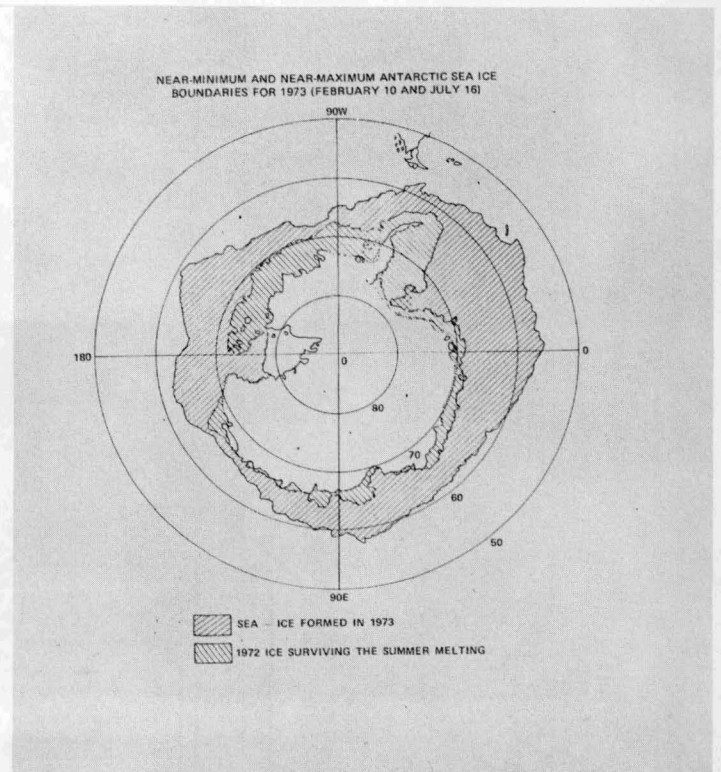


FIGURE 11. Seasonal variations of sea ice in the southern hemisphere.

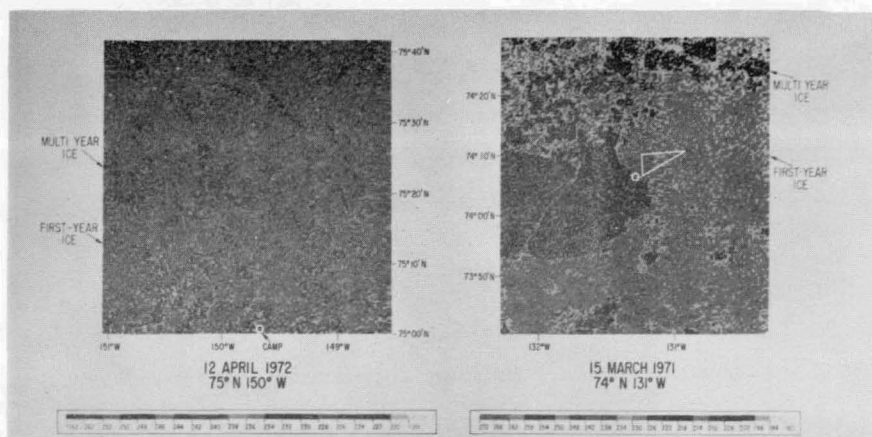


FIG 5

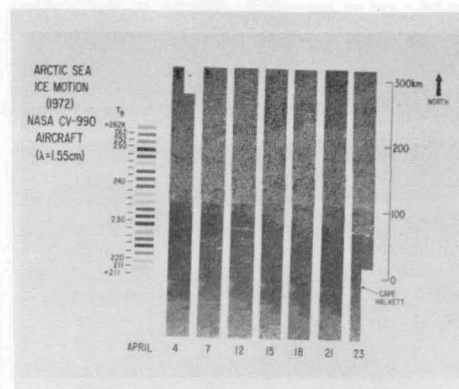


FIG 6

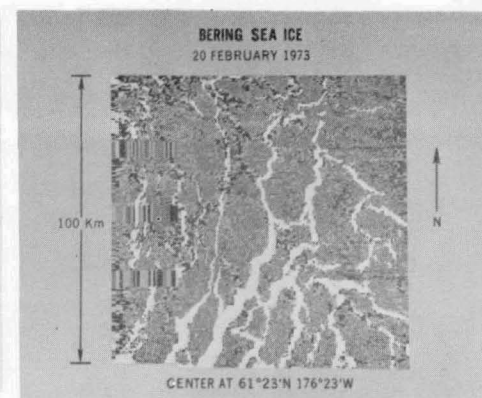


FIG 7

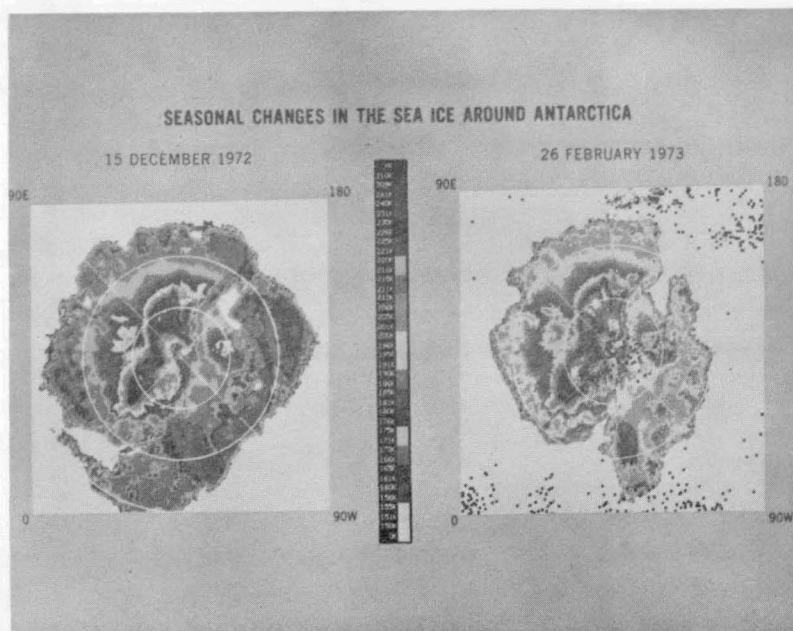


FIG 8

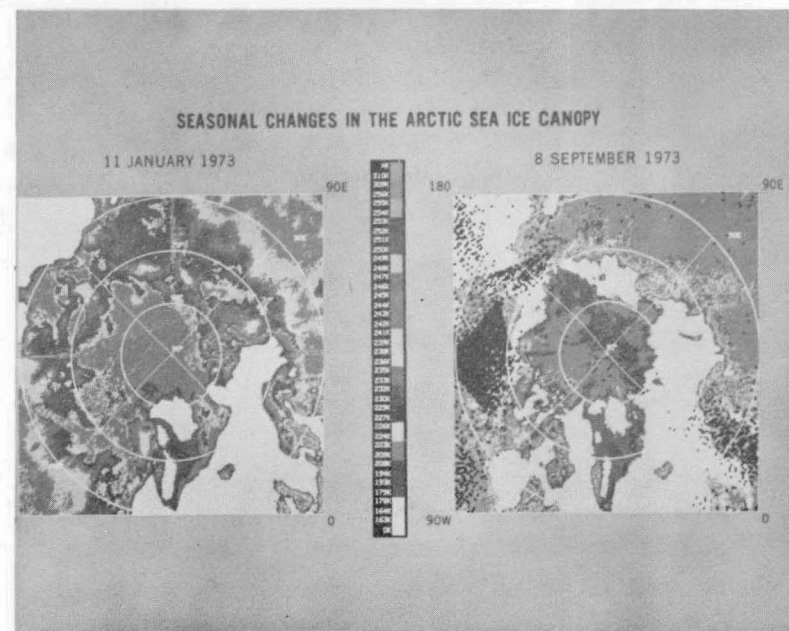


FIG 10

FIGURE 5. False-color ESMR images ( $\lambda=1.55$  cm) collected on the NASA CV-990 aircraft over the AIDJEX areas, Beaufort Sea.

FIGURE 6. Successive false-color ESMR image strips collected between 4 and 23 April 1972 of sea ice of the western Beaufort Sea from Harrison Bay, Alaska to  $74^{\circ}\text{N}$ .

FIGURE 7. False-color ESMR image collected on 20 February 1973 on NASA CV-990 aircraft over the BESEX area, Bering Sea. The image is centered near  $61^{\circ} 24'\text{N}$ ,  $176^{\circ} 24'\text{W}$ .

FIGURE 8. False-color ESMR mosaics collected over the northern hemisphere on 11 January 1973 and 8 September 1973 depicting seasonal changes in the Arctic sea ice canopy.

FIGURE 10. False-color ESMR mosaics collected over the southern hemisphere on 15 December 1972 and 26 February 1973 depicting seasonal changes in the Antarctic Sea ice canopy.



FIGURE 12. SLR image of AIDJEX area taken by DND Argus Aircraft with a Motorola AN/APS real aperture radar during April 1975. The dark spot in the center of the image is the AIDJEX camp "Big Bear". Light areas indicate low returns and dark areas indicate high returns. Image was taken by the port antenna with the aircraft flying in a northerly direction.



FIGURE 13. SLR image of McKenzie Delta area taken by the DND Argus aircraft with a Motorola AN/APS 94D real aperture radar during April 1975. Image was taken by the port antenna with the aircraft flying in a northerly direction. Light areas indicate low return and dark areas high returns. Note the man made disturbances of the snow cover on the shore fast ice at the beginning of the image. Black lines across the image are time reference marks.



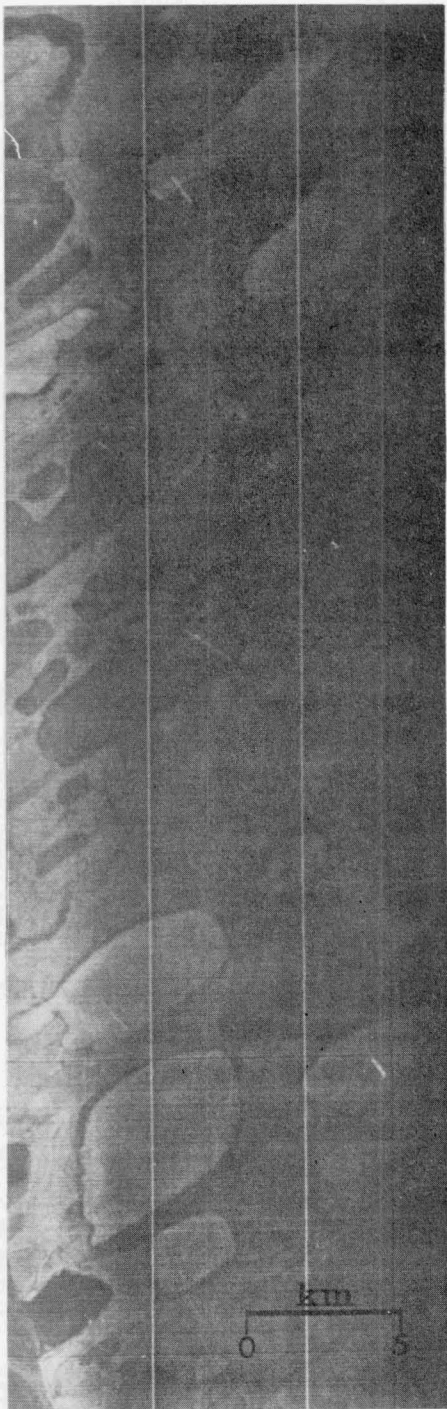


FIGURE 15. SLR image of area just west of Harrison Bay, Alaska taken by a U.S.G.S. Mohawk aircraft with a Motorola AN/APS 94XE1 real aperture radar during April 1974. The image includes Naluakruk, Okalik and part of Teshekpuk Lakes. Note the differences in radar return from lakes which at the time the image was made were covered with 2m of ice (Sellman et al., 1975).

FIGURE 16. SLR image with McKenzie Delta channels and lakes taken by the DND Argus aircraft with a Motorola AN/APS 94D real aperture radar in April 1975. Image was taken by the port antenna which was used to image the main channel twice at 90° to each other. The light areas indicate low returns and the dark areas indicate high returns.



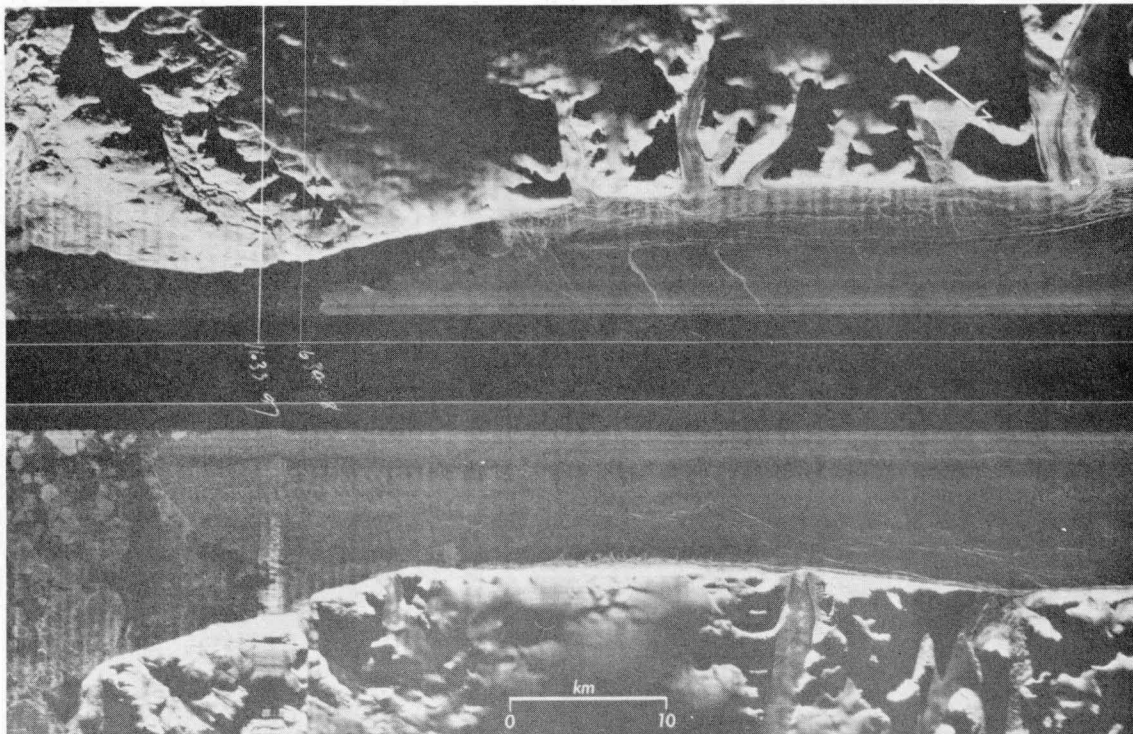


FIGURE 17. SLR image of Peterman Glacier, northwest Greenland taken by the DND Argus aircraft with a Motorola AN/APS 94D real aperture radar in March 1975. Dark areas indicate high returns and light areas low returns. The aircraft was flying in an easterly direction.

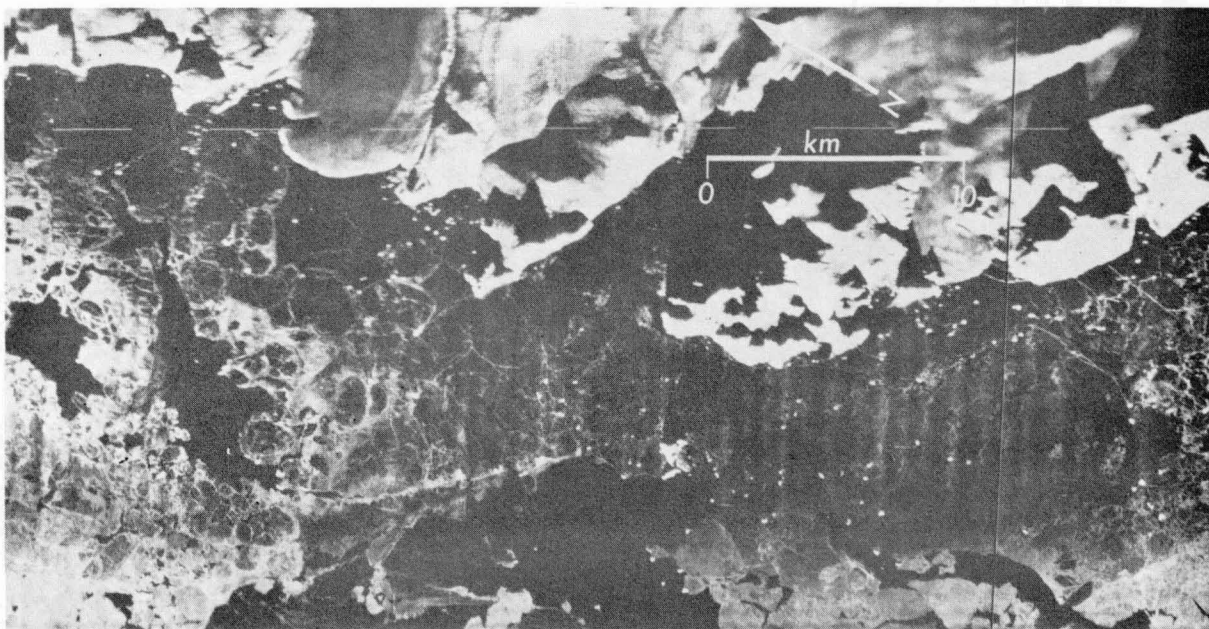


FIGURE 18. SLR image of icebergs off the coast of Cape Atholl, near Thule, Greenland taken by the DND Argus aircraft with a Motorola AN/APS 94D real aperture radar in March 1975. Dark areas indicate low returns and light areas high returns. The image was taken by the port antenna while the aircraft was flying in a southerly direction.

FIGURE 19a

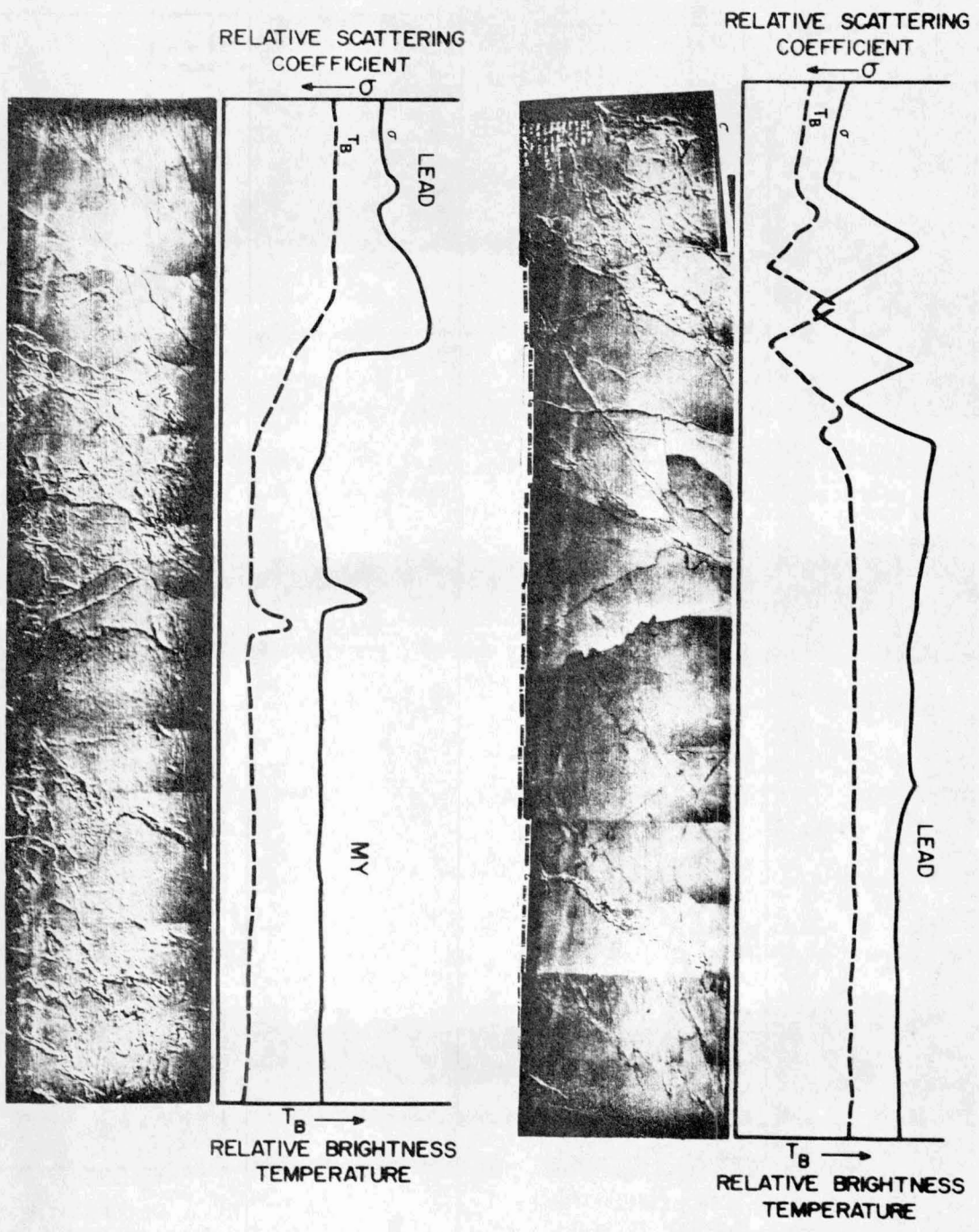


FIGURE 19b

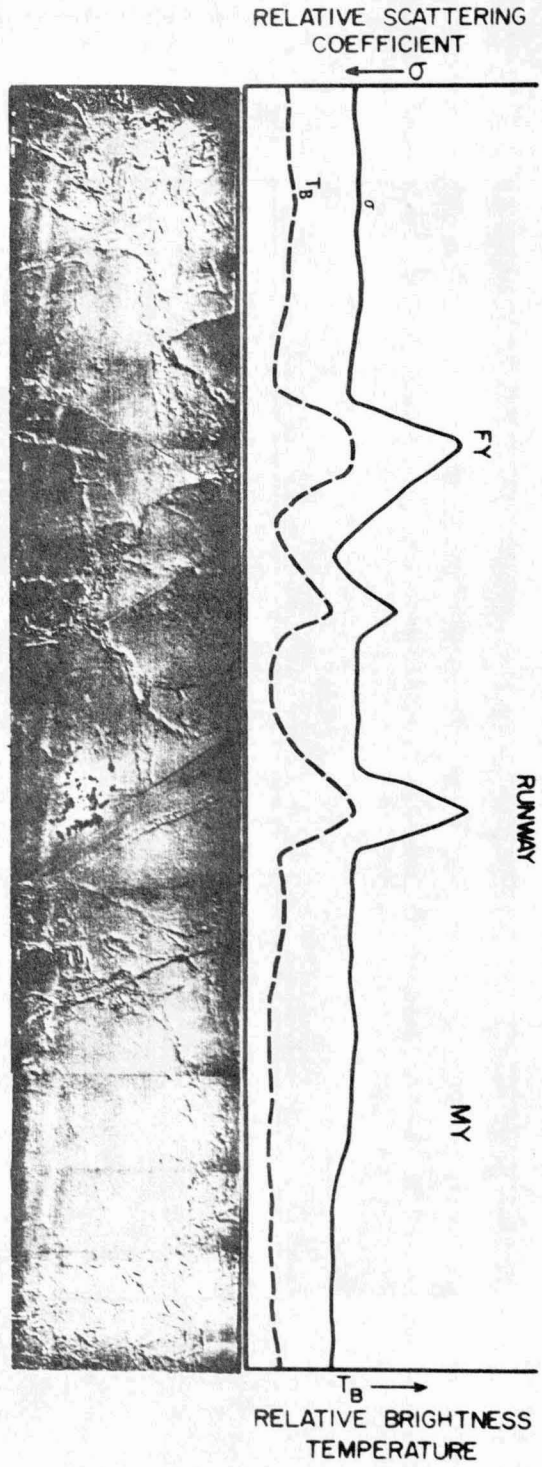
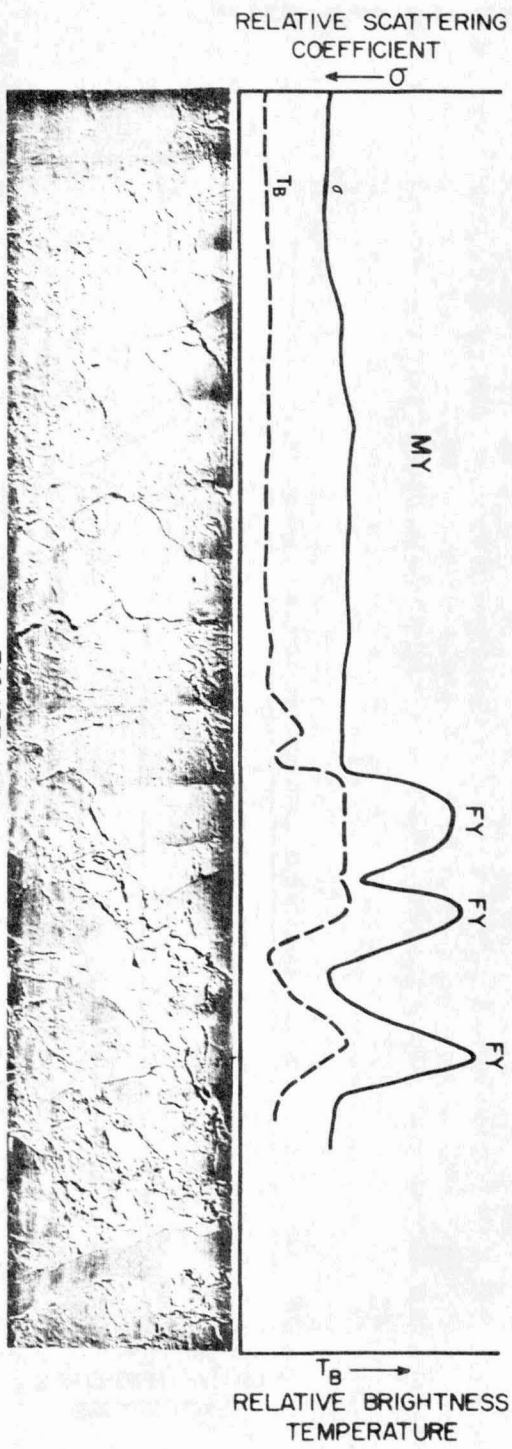
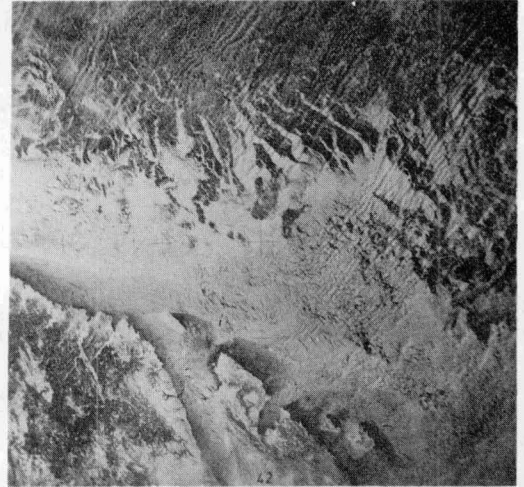


FIGURE 20. SKYLAB-4 images taken by the astronauts over the Gulf of St. Lawrence.



(a) 11 January 1974, NE part of Gulf of St. Lawrence, Straits of Belle Isle. Note the frazil ice plumes parallel to the wind direction.



(b) 19 January 1974, NE part of Gulf of St. Lawrence, Straits of Belle Isle. Note the consolidated ice pack and ice plumes perpendicular to the wind direction.

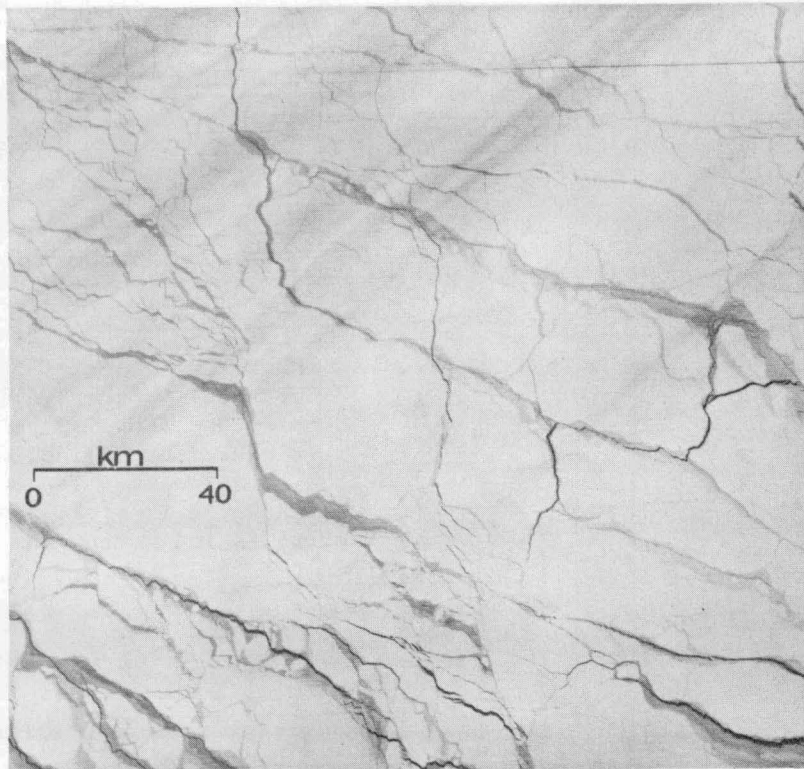


FIGURE 21. LANDSAT (MSS-7) image of pack ice in the central Beaufort Sea ( $77^{\circ} 52'N$ ,  $138^{\circ} 04'W$ , 30 March 1975). The image is 185 km on a side.

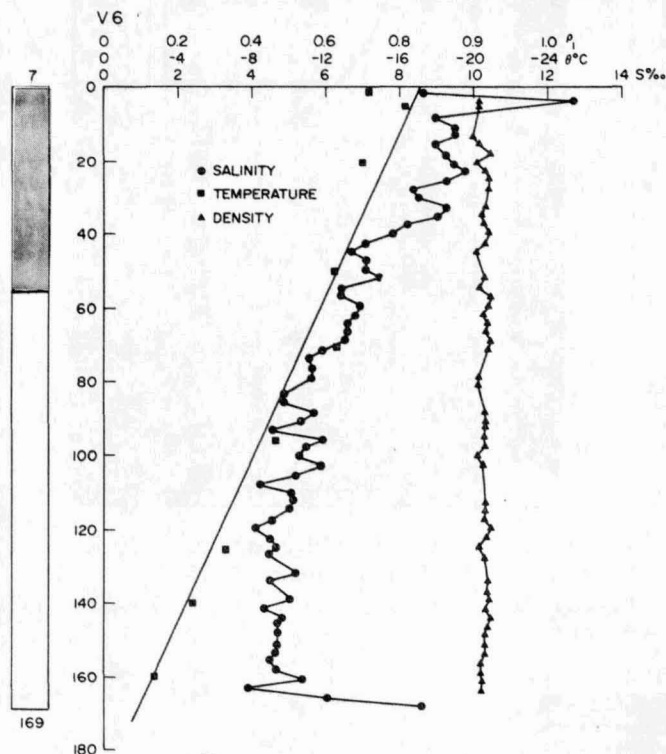
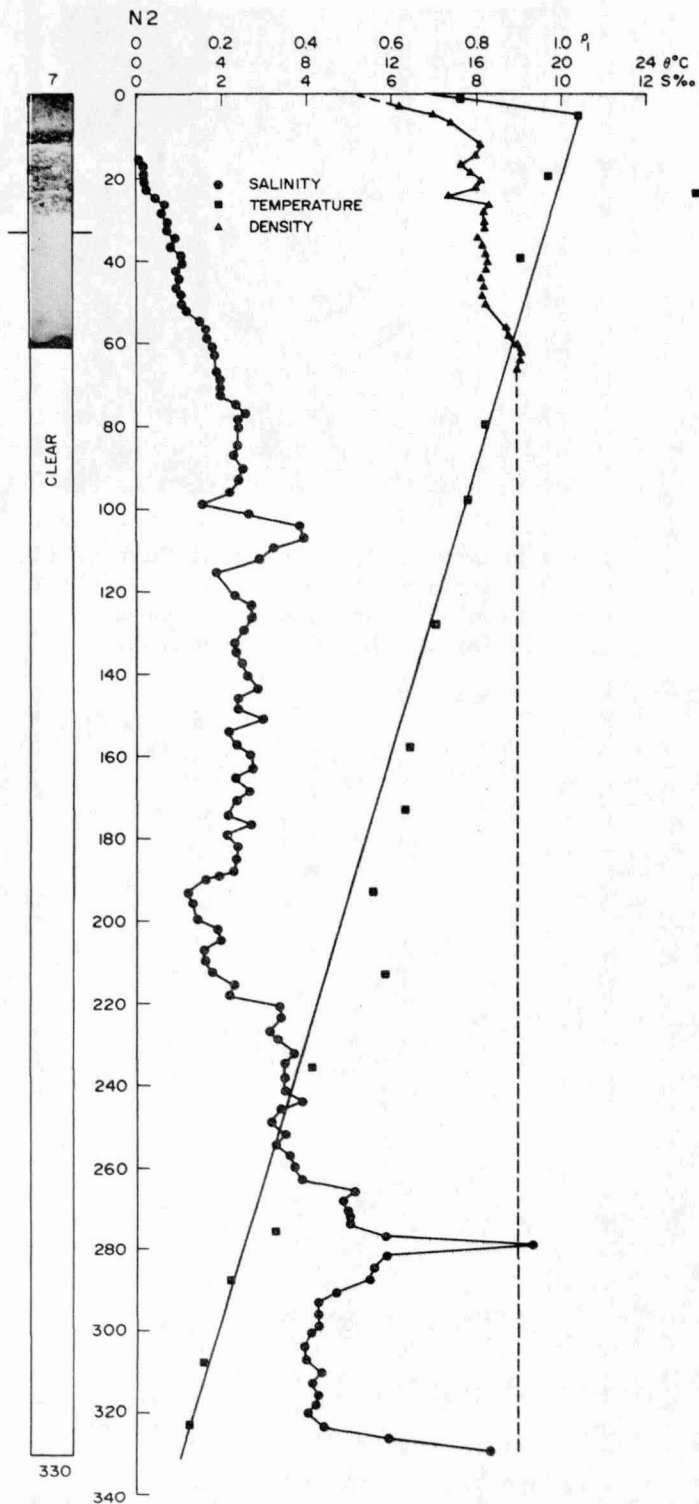


FIGURE 23. Depth profiles of salinity, density and temperature for first-year and multiyear ice obtained during April 1975 at the AIDJEX camp. The schematic of the core is shown on the left hand side of the profiles indicating the structural changes in the ice cover.

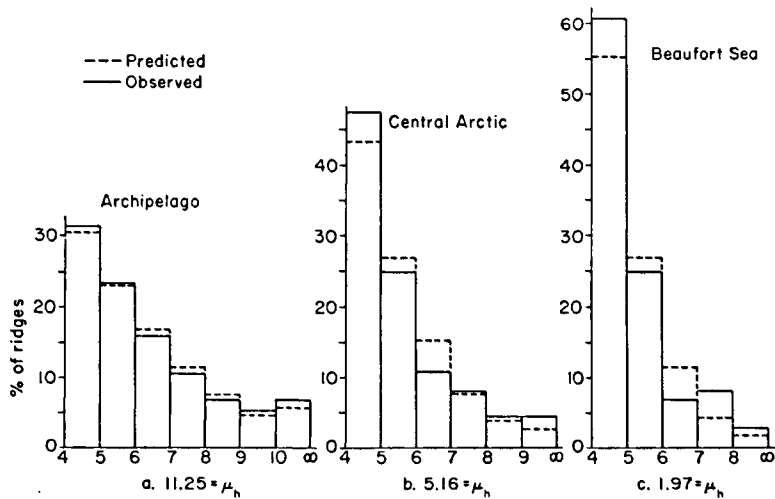


FIGURE 22. Ridge height distributions taken in February 1973. Each distribution was taken from a laser track approximately 40 km in length and the average number of ridges per kilometer above 4 ft (1.22 m) is denoted by  $\mu_h$  for each distribution. The two parameter fit is indicated by dashed lines with the actual data being solid. Distribution a, was observed at approximately lat.  $83^\circ\text{N}$ , long.  $85^\circ\text{W}$ ., b at lat.  $87^\circ\text{N}$ ., long.  $162^\circ\text{W}$ ., c at lat.  $70^\circ\text{N}$ ., long.  $139^\circ\text{W}$ . The mean ridge heights for distributions a, b and c were 1.93 m, 1.70 m, and 1.57 m respectively (Hibler, 1975).

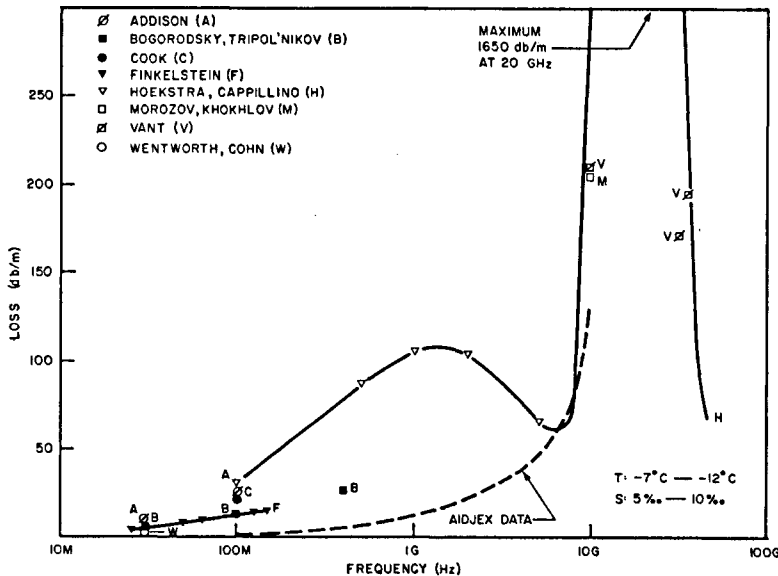


FIGURE 24. Summary of the dielectric loss data for ice of a standard salinity and of a standard temperature. The dashed line indicates the trend of the 1975 AIDJEX results obtained by Vant (personal communication).